ADDIS ABABA UNIVERSITY

School of Graduate Studies

College of Natural and Computational Sciences

Characterization of the heat source of Butajira geothermal field Ethiopia: noble gas approach

A thesis

Submitted to

The School of Graduate Studies

of Addis Ababa University

In partial fulfillment of the requirements for the Degree of

Masters in Geothermal Energy

Yared Sinetebeb

May 2019

Addis Ababa University School of Graduate Studies

This is to certify that the thesis prepared by Yared Sinetebeb, entitled: Characterization of the heat source in Butajira geothermal field, Ethiopia: noble gas approach submitted in partial fulfillment of the requirements for the Degree of Master of Science in Geothermal Energy complies with the regulations of the University and meets the accepted standards with respect to originality and quality.

Signed by the Examining Committee:

Examiner - Signature _____Date_____

Examiner: Signature_____ Date_____

Advisor:
Gezahegn Yirgu (Professor) _____Date _____

Co-Advisor:
Peter Barry (PhD) _____Date _____

Abstract

Butajira geothermal prospect is found in the Central Main Ethiopian Rift (CMER) near the western escarpment where thermal manifestations such as hot springs are aligned along NNE/SSW direction with surface temperature reaching up to 86°c are located. Hydrothermal alteration materials in the area, the chemistry of the fluids, the source of heat that drives the geothermal system as well as the sub surface reservoir temperature is not well defined. The main objective of this study is to provide constraints on the heat source and to estimate the reservoir temperature using volatile elements like helium as well as to estimate reservoir temperature using cation geothermometers. As a result sub surface temperature exceeding 150°c is obtained using Na-K geothermometer and the measured ratio of $^{3}He/^{4}He$ shows broadly consistent value of 2.3Ra indicating 12% of plume signature and 88% of crustal origin referring to a very high crustal contamination probably derived from well evolved stagnant magma chamber at relatively shallow depth.

Acknowledgment

I would like to thank my advisors Professor Gezahegn Yirgu and Dr Peter Barry for their continuous follow up, feedback and comments that support me a lot in making a good progress in the research. Especial gratitude is addressed to Peter Barry that helps me a lot in collecting as well as analyzing the gas samples. The Department of Chemistry at Addis Ababa University is also acknowledged for doing the cation analysis of the water samples.

Table of contents

List of Figures

List of Tables

1. Introduction

1.1 Background

Access to energy is among the key elements for the economic and social developments of a country. In a developing country like Ethiopia, long term electrical generation development plan consists mainly of hydro projects. Hydropower generates more than 90% of electricity in Ethiopia but to ensure sustainable energy supply, the country needs to diversify its energy policy. Since recent times, Ethiopia has shifted its policy from relying in a single source of electric power (hydro) to other sources of energy. There is critical concern about the climate change and one of the least pollutant forms of energy is geothermal energy. Geothermal energy is considered as renewable form of energy by referring to the sustainable rate of energy recharge. This thermal energy within the interior of the earth is enormous and could last for several millions of years. The source of heat inside the earth is mainly derived either from the residual heat during accretion or from heat released during radioactivity process. It continuously flows through conductive transfer or through convective flow of the underlying mantle. Although volcanic activity could bring substantial amount of heat to the surface not all of its volume reaches the surface rather left underneath driving hydrological convection to form high temperature geothermal reservoir. Reservoir within the Earth from which heat can be economically extracted is considered as a geothermal resource (Gupta and Roy, 2006). The enormous heat potential of the earth can be evidenced from hydrothermal manifestations such as hot springs and fumaroles at the surface. Due to the tectonic setting and the volcanic activity throughout the Ethiopian rift, different geothermal prospects have been identified. The high thermal gradient and the relative ease of fluid flow leads to the creation of high temperature geothermal areas. Among these some are in a feasibility stage but many of them are still in the exploration phase. Geothermal resource exploration and long term development for generating electricity as well as for direct utilization is recently getting various support and attention in the country from both the government and the private sectors.

1.2. Geographic setting of the Study Area

1.2.1. Location and Accessibility

The study area is found in the (CMER) about 150 km South of Addis. It is found under the Southern Nation, Nationality and People Regional state (SNNPR) with in the Silti zone. It is accessible via two ways one is through Ayer Tena in Addis to Tiya, Kela, Butagira and Silti while the other is from Addis to Debre Zeyt, Ziway, Butajira and Silti. The area is covered by several hot springs and mud pools following a similar lineament of NNE/SSW direction. The CMER is in some kind of transition phase where localized strain is shifting from the margins toward the rift floor (Agostini et al, 2010). Rift margin geology is dominated by volcanic rocks of the Tertiary Period (WoldeGebriel et al, 1990). The study area is found near the Western Escarpment of the Guraghe highlands. This Western Escarpment is exposed with a very thin and scarce crystalline basement, identified as

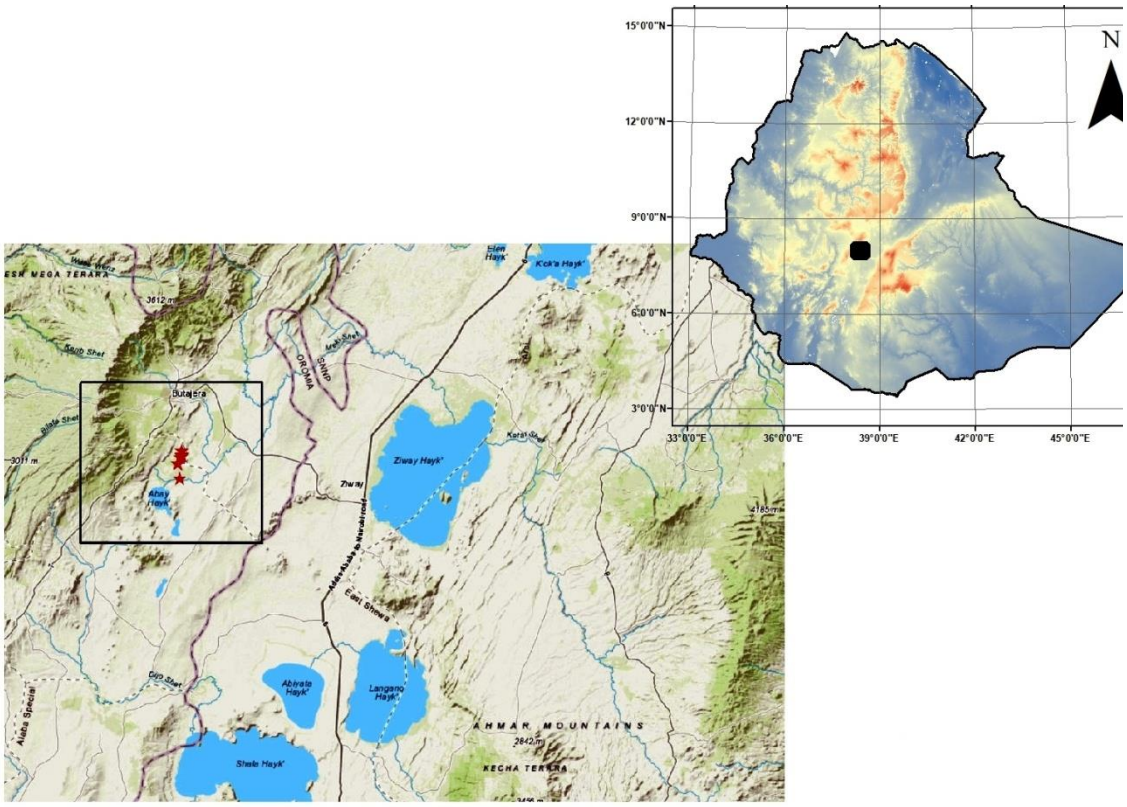

Figure 1. Location map of the study area in black box where red stars indicate the site of thermal manifestations

biotite gneiss intruded by quartzofeldspathic pegmatites, which is overlain by thinner Mesozoic sediments that comprises the Adigrat sandstone and the Antalo limestone all covered by thick piles of Pre- rift Tertiary basaltic rocks (WoldeGebriel et al, 1990).

1.2.2. Weather and Climate conditions

The climate and weather conditions in Butajira and its surrounding areas have been categorized in tropical zone. The season from October to February is relatively dry and windy. The rainy seasons are from March up to September where highest rainfall rate occurs during July and August where 163mm is recorded. The average annual temperature is 24°c. January is regarded as the hottest month of the year having low temperature up to 17°c. The average annual precipitation in Butajira is 105mm.

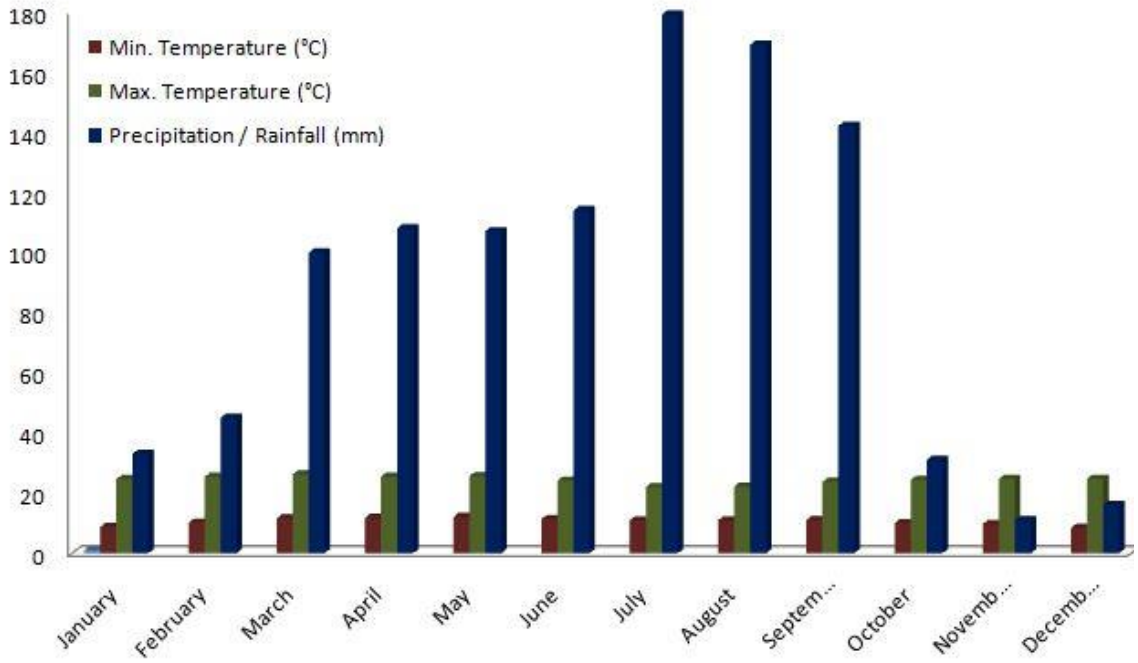

Figure 2. Bar graph showing the climate and weather conditions of Butajira area against months of a year downloaded from https://en.climate-data.org/africa/ethiopia/southern-nations/butajira-31830/

1.2.3. Physiography and Drainage system

The area is bounded by the Guraghe highlands from the West that are elevated more than 3000m asl and different rivers and streams flow towards East where almost all meet at the lowest elevation of 1820m at Lake Abaya as shown in figure 3. In fact the area is largely exposed to flooding. Further going to the rift floor, there are structures following NNE/SSW and NW/SE direction in which the major rivers follow these structures. Almost all rivers are seasonal.

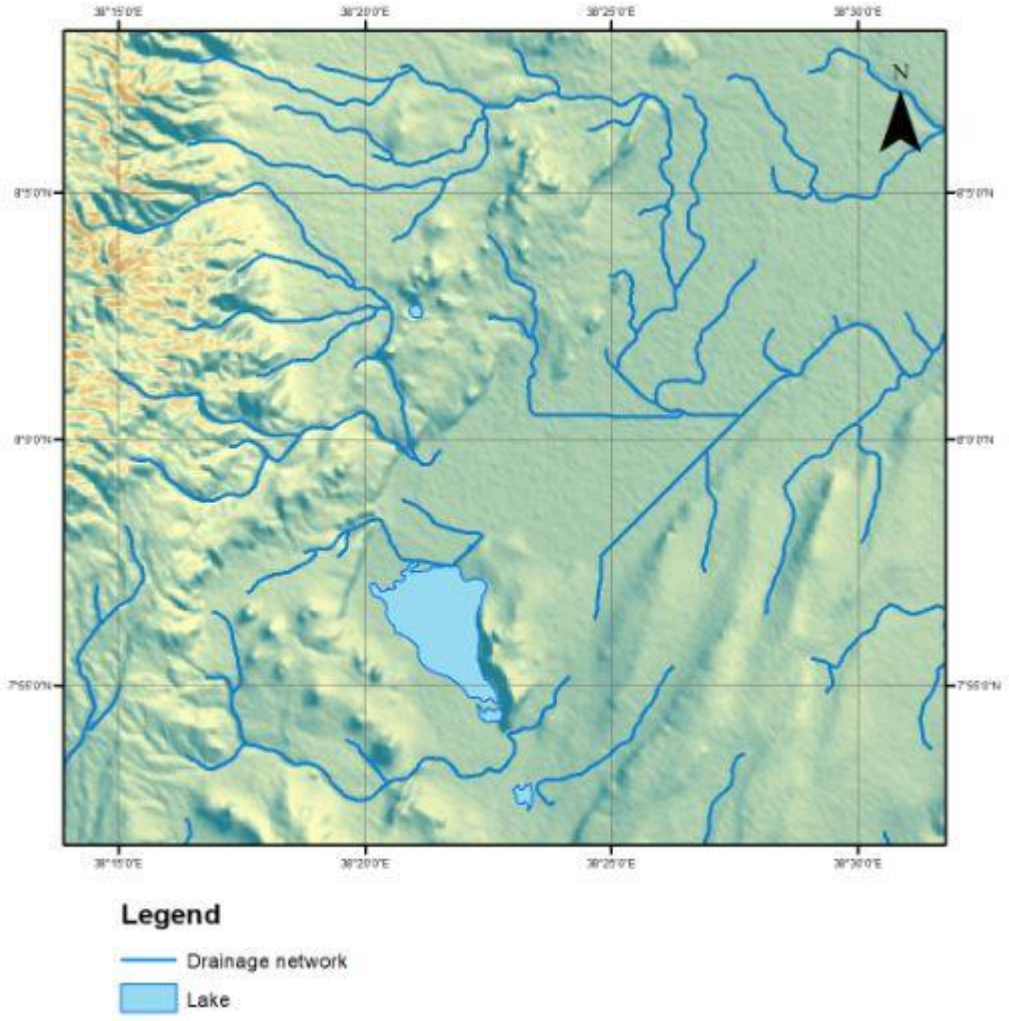

Figure 3. Drainage network of Butajira geothermal field

1.2.4. Problem Statement

Various researches and studies have been investigated in the CMER and many of them are presented in the sub-chapter of literature review. Most geothermal prospects in the Ethiopian rift especially of the high enthalpy geothermal fields are found along the central axis. The study area, near the western escarpment, did not receive proper attention in terms of its geothermal potential other than the existence of warm springs of 48°c temperature mentioned by Di Paola (1973) and she insisted to undertake further investigation in the area. Recently a sudden blowout of high temperature steam occurred in a shallow well drilled for ground water exploration and the area has been given attention about its geothermal activity since then. The scientific problems that can be outlined are for example detail geological and structural map is not readily available. The volcanic history and timing of the various eruptive centers is not well understood. The source of heat and the chemistry of the fluids is not well defined. Information about the hydrothermal alteration products and the reservoir characteristic is not properly constrained.

1.3. Objectives

1.3.1. General Objective

The principal objective of this research is to characterize the heat source of Butajira geothermal prospect.

1.3.2. Specific Objectives

- Describe the volcanic geology and tectonics in detail
- Define and characterize the origin of the heat source in association with recent volcano tectonic activity in the area
- Describe the thermal manifestations in the area and estimate the sub surface reservoir temperature
- Determine the provenance of volatiles

1.3.3. Expected outcomes

The result of this research and its findings will help in identifying the possible source of heat of the geothermal fluids. The sub surface reservoir temperature will be estimated using cation geothermometer. The provenance of volatiles will be determined. In fact the findings of this research will provide original data and interpretation leading to a better understanding of the Butajira geothermal system thus promotes and encourage exploration work in geothermal prospecting in the area.

2. Previous work on the MER

There are quite different works conducted within the Main Ethiopian Rift (MER). The evolution of rifting, propagation and localization of active deformational zones has been investigated using geological, geochemical and geophysical approaches. Several geological units of the MER, Quaternary volcanism, and age of the tectonic structures associated and their orientation was discussed by the pioneer geoscientists like Mohr (1962). In this study focus on recently published articles are well included.

2.1Geological and geochemical overview

WoldeGabriel et al (1990) managed to do petrography and K/Ar dating from rocks exposed in both sides of the rift escarpments and provides the stratigraphic chronology of the CMER. According to the chronology they put from Oligocene up to recent, there have been six sequences of volcanism and they tried to classify and show the development of the rift in two different phases. The existence of recent basaltic lava flows in Butajira, East Ziway and Southern Shala associated with fissural scoria cones are reported also by Di Paola (1973). Various base and precious metals like chromium and gold more than 21ppm and 0.06ppm respectively were reported to be found around Butajira and its surrounding areas from geological and geochemical approaches (GSE, 2010). Agostini et al (2011) conduct ^{14}C radiometric dating on rocks that are affected by faulting from both rift margins and shows that the youngest border faults to be 30ka for the western and 7-9ka for the eastern escarpment. Keranen and Klemperer (2008) indicate that rift propagation is controlled and largely dependent on preexisting structures. They concluded that rift development is credited by tectonical structures at earlier times and recently dominated by magmatism. From fault kinematics, petrology and satellite image analysis Bonini et al (2005) suggested that rift propagation is towards south. They argue that after the initiation of the Southern Main Ethiopian Rift (SMER) and Northern Main Ethiopian Rift (NMER) from 20-21Ma and 11Ma respectively the deformation ceased to continue further north probably due to pre-existing transversal structures. From exposed basement rock located in the CMER Tsegaye Abebe et al (2010) conducted apatite fission track and emphasize the model proposed by Bonini et al (2010) conforming the age of CMER to be younger than 8Ma. Structural and geological as well as GPS data analysis in the CMER reveals that both faulting, provoked by magma, and pre historic tectonical structures, caused by earthquakes, have been accounted to be responsible for strain accommodation (Pizzi et al., 2006). Isotopic ratio as well as major and trace element modelling conducted in the flanks and

floor of the NMER shows that the difference in the composition of silicic products directly depends on their primordial original source of the magma and degree of fractionation (Kabeto et al., 2009). They concluded that acidic rocks along the border have alkaline type magma as a source while silicic products of the rift floor have transitional basaltic source that undergoes higher degree of fractionation than the rocks at the margin. From geochemical perspective Rooney et al (2007) reports that the magmatic system is better developed along the Wonji Fault Belt (WFB) than underneath the Silti Debre Zeit Fault Zone (SDFZ). Moreover the fractionation depth of the magma in eastern escarpment is at shallower depth while magmas at SDFZ are from deeper fractionation depth (Rooney, 2010). He also conclude that there is a clear relationship between tectonics and magmatism from major and trace element analysis on the basaltic lavas from the recent structure of WFB and SDFZ. Xenoliths inclusion in the lavas of Butajira has showed to contain Al-augite which is widespread along the youngest deformation zones of SDFZ and WFB implying the event of dyking in to the crust to a depth of 30km (Rooney et al., 2005). Using major and trace element isotopic analysis on the very recent (<1Ma) basaltic lava fields of Debre Zeyt and Butajira area Rooney et al (2012) concludes that there is clear discrepancy in the original source of the isotopes analyzed. They insist that there is mixing between the asthenospheric upper mantle, the diverging continental lithosphere as well as contribution from deep seated plume. From radiometric, petrographic and structural data Tsegaye Abebe et al (1998) suggests on the volcanism of Yerer Tulu Wellel Lineament (YTVL), E-W trending transtensional structure, to be controlled by both regional structural effect and also by anomalous heat from the MER. It has been shown that there are variations in the evolution of highly differentiated rocks and to take care in using Sr isotope methodology (Deniel, 2009). The reason for the observed discrepancy of rock compositions from Gedemsa volcano were petrochemicaly analyzed (Peccerillo et al., 2003). They have interpreted the variation by saying that silica rich evolved products can be fractionated from mafic magmas and explain the paucity of intermediate rocks due to short temperature interval associated with the collapse of the caldera. Hutchison et al (2016) also indicates the genetical origin of the rocks from Gedemsa to be predominantly affected by fractionation processes. Fractionation process has been reported to play the major role in producing variation in composition of rocks erupted from the same vent as it is observed in the petrogenesis from lavas of pre and post caldera formation of Fentale volcano (Gibson, 1972). Minissale et al (2017) conducted geochemical investigation in the SMER using $^{3}He/^{4}He$ isotopic ratio and geothermometery application in Northern Abaya and reveals

both the equilibrium temperature of the reservoir as well as the source of origin for the thermal fluids.

2.2Geophysical overview

The contribution of mantle upwelling and the effect of the Mid Oceanic Ridge (MOR) along with the variation in the physical properties of several types of rocks are said to be the major cause of rifting in East Africa as shown in the spherical shell stress model of Min and Hou (2018). Whaler and Hautot (2006) provide resistive structure of the crust beneath Boset volcanic complex and revealed the presence of magmatic chamber at 20km depth by using audio-frequency Magneto Telluric measurements. Cornwell et al (2006) also confirm in their density model beneath Boset volcanic center that there is mafic intrusion at around 20km depth. Velocity modeling conducted along a profile that transects the MER through Boset volcano suggests higher velocity values to be found within the rift presumably due to magmatic intrusions than in the plateaus (Mackenzie et al., 2005). Seismic refraction method conducted in the NMER showed that the P-wave velocity increases under the rift axis than underneath the margins (Maguire et al., 2006). Bastow et al (2000) insists for the cause of strain accommodation in NMER to be predominantly magmatic intrusion as observed from tomographic inversion of P and S wave data. Furthermore using geodesy combined with fault slip inversion data Ameha Muluneh et al (2014) concludes that left lateral transtensional component is responsible for the propagation and evolution of the Ethiopian rift. They have suggested the sigmoidal shape of the Quaternary WFB as evidence. Recent (MT) resistivity models conducted around Aluto suggests that the cause of unrest in Aluto is not driven by the action of shallow magmatic system (Samrock et al., 2015). They rather concluded the occurrence of substantial melt at relatively shallower depth to be found along SDFZ.

2.3 Geothermal Development in Ethiopia

Geothermal resource in Ethiopia is becoming one of the most favorable alternative sources of energy. Ethiopia has been taken a long and tedious journey to develop and generate power from its huge thermal potential. United Nation Development Program (UNDP) was the first to search for areas with active geothermal fields within the Ethiopian rift by the request of the Imperial government in 1970. Active geothermal resources tend to be found along major plate boundaries. Accordingly from geological, geochemical and geophysical techniques conducted major hydrothermal areas were delineated and detail regional map was established (UNDP, 1973). Hydrothermal areas of the Lake District of the MER and

Afar region, their water type, tectonical setting was formulated thus around 120 localities have been identified to have an independent circulation system (UNDP, 1973). The occurrence of low temperature fluids in Ethiopian rift and its application has been compiled (MOM, 1984). In 1986 Electro Consult (ELC) and Geological Survey of Ethiopia conduct various reconnaissance geoscientific investigations in central and southern Afar (Solomon Kebede, 2016). Investigations by ELC focused primarily on Tulu Moye, Dofan, Bossetti, Fentale and Gedemsa from the MER Teo, Danab, Meteka and Lake Abe from the Afar rift (Zewde Gebregziabher, 1997). Prospects such as Aluto, Corbeti, Tendaho and Abaya were given more priority than the others to proceed for drilling phase (Tsegaye Abebe, 2000). Eight exploratory wells were drilled in the 1980s in the central sector of the MER particularly at Aluto, huge silicic center between Lake Ziway and Lake Langano, and five of them were productive with recorded enthalpy up to 1650 kj/kg (Tsegaye Abebe, 2000). A 7.3 MWe net capacity pilot plant was installed in Aluto in 1998 although it is not functioning due to technical difficulties (Solomon Kebede, 2016). Recently two appraisal trajectory wells with temperature above 300˚c were drilled in the up flow zone of Aluto for the purpose of reservoir modeling. Discharge tests showed that 5MWe could be generated out of these two wells (Solomon Kebede, 2016).

Exploration drilling was also conducted in the Tendaho graben in Afar from 1993-1998 and high temperature fluid above 250c was tapped at relatively shallow depth (Solomon Kebede, 2016). The geothermal resource in Afar is more promising than the MER although it is not well exploited. This is due to the non-availability of adequate infrastructure and the faraway of the fields from the national grid (Solomon Kebede, 2016). Geothermal resource development in Ethiopia is localized to few regions because of none availability of permeable structures (Tsegaye Abebe, 2000). He also mentioned that the elevated topography of the rift axis and regional drainage flow away from the rift give rise to poor recharge zones. Tulu Moye is another prospect that has been studied well. Ministry of Mines and Energy (MOM) conduct various geoscientific surveys in Tulu Moye.. This peralkaline silicic lava with not more than 0.8 million year of eruption history is covered by highly evolved products like rhyolites and ignimbrites that are highly fractured by NNE/SSW faults of Wonji group and NNW/SSE transverse faults (MOM, 2008).

Three individual sectors with hydrothermal manifestations depicting high permeable zones are identified using mercury and radon survey (MOM, 2008). Recently Japan International Cooperation Agency (JICA) together with the collaboration of GSE has already established

geothermal master plan study for 22 fields that are regarded as high enthalpy geothermal prospects. Their study reveals the potential of the Ethiopian rift to possess up to 10800 MWe (Solomon Kebede, 2016).

3. Regional geological setting

Continental rifting leading to the formation of oceanic basin makes East Africa an important place Keranen and Klemperer (2007) to achieve basic understanding of rift evolution (Agostini et al., 2011; Corti, 2009 ; Beccaluva et al., 2009; Giordano et al., 2014; Furman et al., 2004 and Chorowicz, 2005). The East African Rift System (EARS) has two branches one comprised with both volcanism and tectonics while the other is predominantly affected by tectonics only. The former is considered as the Eastern branch and the latter is called the Western arm (Chorowicz, 2005). In contrast with the western branch, the evolution of the eastern rift is largely induced by swelling of magma that causes the lithosphere to break than the far field crustal extension (Kendall et al., 2005). The climatic and environmental change around the equator has been hypothesized to be affected as a result of impinging mantle plume (Abbate et al 2015; Wichura, 2010). Volcanism has been occurred since the time of Oligocene (Peccerillo et al., 2003; Corti et al., 2010). Before the Oligocene the surface relief of Ethiopia is not elevated only covered by Cretaceous deposits then during Oligocene eruption of flood basalts begins (Abbate et al., 2015). For the extensional deformation and associated rifting in East Africa, the thermal uplift is thoroughly considered to be the cause (Getahun Demissie, 2010). Other than intruding magma the constant elongation and divergence of the lithosphere can and will trigger the underlying asthenosphere to bulge (Mohr, 1992). This upwelling of the asthenosphere results in thinning of the crust reducing from 38-51km in the plateaus to 31km within the rift (Mahatsente et al., 1999). The effect of underlying mantle plume intruding in the Eocene Oligocene times Wichura (2010), the consequent deposition of the trap basalts and uplifts causes the elevated topography of present day Ethiopia (Abbate et al., 2015).

The first opening of rifting was caused by the effect of plume intrusion around 30Ma (Chorowicz, 2005). Initiation of rifting succeeds and lies on previous structures made by orogenic processes of the Precambrian era (Getahun Demissie, 2010; Chorowicz, 2005; Corti, 2009). From 5-9Ma and especially since 2Ma extension accompanying by subsidence and thermal upwelling plays a major role in the development and evolution of the rift (Macgregor, 2015). In addition to that, variations in the African basement together

with Atlantic and Indian oceanic spreading ridges also provide significant contribution for the initiation of the East African rift (Min and Hou, 2018). According to Giday WoldeGabriel et al (1990) the development of rift formation has transformed from incipient half grabens to fully developed rift formation during Miocene to Pliocene. From fault slip data and radiometric C14 dating (Agostini et al, 2011) rift maturity and crustal modification has been reported to decrease from North to South (Bonini et al., 2005; Corti et al., 2010; Corti et al., 2013; Keranen and Klemperer, 2007). Crustal thickness also reported to decrease further North in to Afar implying the transition zone from continental break up in to oceanic rift formation (Maguire et al., 2006). Although several debates are there about the direction of rift propagation the hypothesis that supports the Southward migration is better accepted (Tsegaye Abebe et al., 2010; Wolfenden et al., 2004; Keranen and Klemperer, 2007). Southward propagation of rifting at 11.5Ma in the NMER has changed direction along the Yerer Tullu Wellel Volcanic Lineament (YTVL). Volcanism away from the rift and localized but segmented zones of deformation has been also largely controlled by transverse structures like the YTVL evidencing for the southward propagation of the rift (Corti et al., 2010). Acocella et al (2002) also proves that the East _West trending structures were formed before the major rift development as its development can be clearly seen in the plateaus than in the rift floor. However change in the regional extension direction facilitates rift propagation towards south around 5-6Ma (Keranen and Klemperer, 2007; Wolfenden et al., 2004).This idea is also supported by Chorowicz (2005) that suggest the direction of rift propagation towards south following preexisting weak zones.

An active extension between the Nubia and Somalia plates result in the opening of the Ethiopian Rift that extends approximately 1000km south of the Afar triple junction to the Kenyan Rift (Agostini et al., 2010, Agostini et al., 2011, Boccaletti et al., 1999, Bonini et al., 2005 and Corti, 2009). The enormously long rift trends in almost N-S direction. The Main Ethiopian Rift (MER) is about 80km wide around its center with a general trend of N-S to NNE/SSW (Abbate et al., 2015). The MER is subdivided in to the Northern Main Ethiopian Rift (NMER), Central Main Ethiopian Rift (CMER) and the Southern Main Ethiopian Rift (SMER) depending on orientation and timing of the faults (Agostini et al., 2011, Bonini et al., 2005 and Corti et al., 2013). In the MER, N/E trending section of East Africa Rift, Tsegaye Abebe (2010) from observing the systematics that the faults follow two divisions can be outlined, the NNE to NE border faults and the NNE/SSW to N/S orienting WFB faults (Boccaletti et al., 1999).Their petrological and geophysical property also varies (Agostini et al., 2011). The three sectors of the MER are in different

evolutionary phases (Giday WoldeGabriel et al., 2000). Deformation was restricted along previous weak zones until the Late Miocene to Pliocene or from 11-2Ma marking the formation of the border faults (Corti, 2009). During Quaternary the so called WFB structures affecting the rift floor Boccaletti et al (1998) trending NNE were formed around 2my ago (Agostini et al., 2011; Corti, 2009). This is due to change in the direction of extension from E-W into NW-SE (Giordano et al, 2014). Using petrographical; and stratigraphical studies it is also mentioned that the stress field changes in the MER around 1.8- 1.6Ma from orthogonal in to oblique faulting (Boccaletti et al., 1999). The oblique rifting of WFB allowing dyking and magma upwelling in accommodation with regional lithospheric extension is assisting for the development of new oceanic crust after the complete breakup of the continental lithosphere (Corti, 2009). During Miocene-Pliocene, marginal faults were formed and since Pleistocene tectonical deformation seems to shift its zone along the rift floor (Corti, 2009). Wolfenden et al (2004) also mentioned the migration and accommodation of strain along the axis to initiate from 6.6 to 3.5Ma. They conclude that since 1.8Ma the evolved silicic centers and the basaltic dyke intruding the rift floor are the products of this localized deformation zone. The well-built communication between localized deformation on the rift floor and the subsequent intrusion and eruption of magma is the major cause that is triggering the final split of the lithosphere (Corti, 2009; Kendall et al., 2005). The boundary faults with large vertical down throw of more than 100m Corti (2013) while the WFB of the rift floor.

shows down throw less than 100m (Hutchison et al., 2015). WFB with fault spacing ranging from 0.5 to 2km has shown high rate of deformation both along the margins and the axis induced by tectonical structures and magmatism respectively (Pizzi et al., 2006).

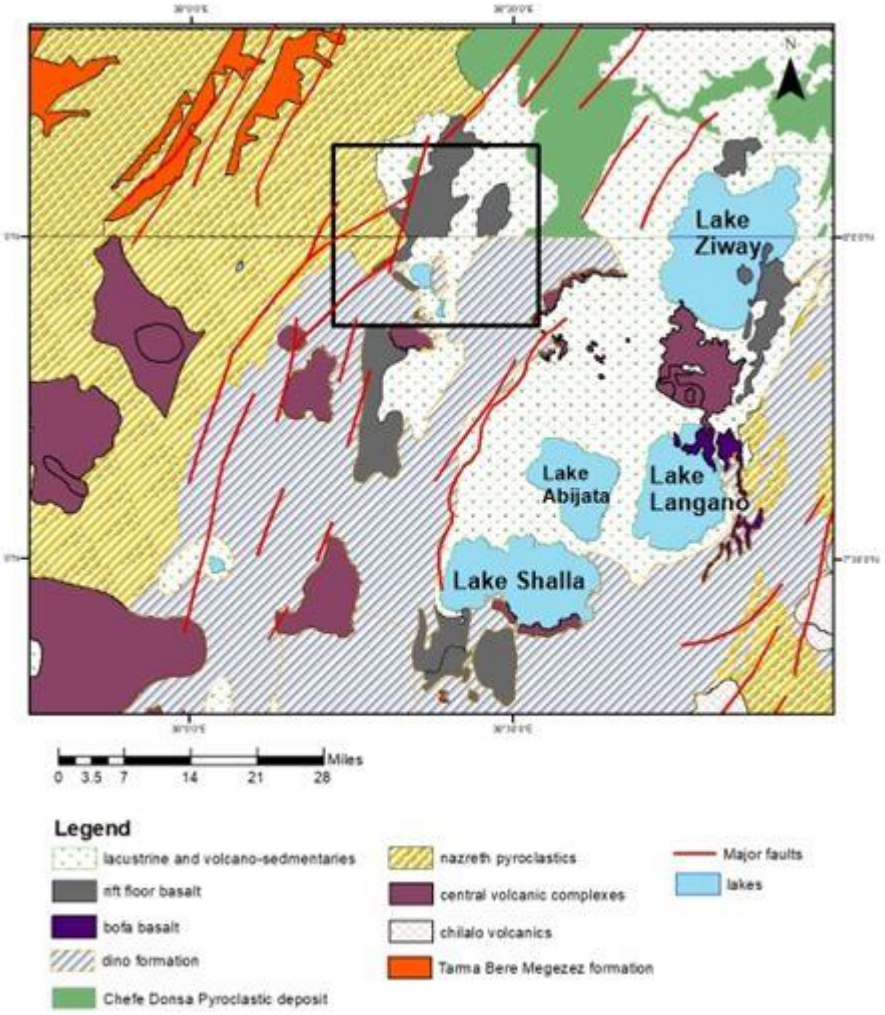

Figure 4. Regional geological map of the MER and major tectonic structures modified from Geological Survey of Ethiopia. black box indicates the location of the study area

Magma controlled rifting Keranen and Klemperer (2007) and its propagation happens in various geological periods where most deformation zones are localized in weakness regions of the Precambrian Era (Corti, 2009; Chorowicz, 2005 and Getahun Demissie, 2010). Thinning of the lithosphere also varies enhancing decompression melt Ring (2014) facilitating volcanism. The cause of magmatism in Eastern Africa is the effect of deep seated super plume according to Halldorsson et al., (2014) and Ring (2014) which initiated at the mantle core boundary (Corti, 2009). Rifting has begun just after the volcanism of flood basalts for example Keranen and Klemperer (2007), Corti (2009) and Ring (2014) where short lived maximum eruption rate has occurred between 31 to 28Ma (Bonini et al,

2005; Corti et al., 2010). The impinging mantle plume is hotter and buoyant than its surrounding which will face decompression melting at its head thus transporting abundant heat through the generation of the flood basalts (Beccaluva et al., 2009). From petrochemical investigation conducted on the volcanics of the MER Brotzu et al (1979) indicates that recent rift basalts are more alkaline than the basalts of the pre-rift formation. The pioneer scientist Mohr (1992) has classified the major lava units in Ethiopia based on their origin. Accordingly alkaline to tholeiitic basalts of the Oligocene indicate a plume source as they are abundant in isotopes of the lithospheric mantle while basalts from Miocene to Pliocene are transitional showing the addition of asthenospheric signature in the lithospheric fraction. Alkalinity has been reported to decrease furthermore as it is indicated by the recently erupted basalts of the Holocene epoch that suggests depleted asthenospheric source (Mohr, 1992). Rocks outcropping in both rift escarpments and the rift floor show bimodality in composition (Boccaletti et al., 1998; Mazzarini et al., 2004; Giordano et al., 2014). The bimodality in composition is achieved when magma undergoes significant fractionation within its chamber and erupts evolved products and also through fractures when primitive magma erupts without fractionating (Gasparon et al., 1993; Tsegaye Abebe, 2000).This is also highly dependent on the strain rate where low strain rate causes wide space fractures resulting in the creation of magma chambers to undergo fractionation while high strain rate with narrow spacing yields fissural basalts (Mazzarini et al., 2004). According to Giday WoldeGabriel et al (1990) ignimbrites, lacustrine products and aligned fissural scoria cones are reported to be found in the Silti-Debre Zeit fault zone (SDFZ) whereas silicic centers are associated along the WFB axis. The depth at which partial melting occurs indirectly infer to the exact pressure at which fractionation begins. Well-developed magmatic system where lava ascends to the surface without noticeable fractionation is depicted along WFB zones than SDFZ where lava fractionation is observed at various crustal depths (Rooney et al., 2007).

Mafic and silicic rocks above Precambrian or Mesozoic sediments are commonly found in the rift floor (Peccerillo et al., 2003). Furthermore transitional rocks such as those found in the NMER and CMER particularly those erupted from Gedemsa and Fentale volcanoes leave evidences that the magma undergoes different fractionation conditions (Giordano et al., 2014). Oldest rocks to be dated around 45Ma are reported to be found in southern Ethiopia (Bonini et al, 2005). The oldest basaltic lava to be sampled in the CMER dates 29Ma and essentially correlated with the trap series of Ethiopia (Bonini et al., 2005). These Oligocene rocks referred as Kela basalts by WoldeGabriel et al (1990) are underlain by

thick Mesozoic sediments and Precambrian rocks. These rocks have aphyric texture with maximum exposed thickness of 150m (Agostini et al., 2011). The volume that the flood basalts hold is about 350000km^3 due to continuous magma supply from the impinging plume underneath (Abbate et al., 2015). These basalts cover large provinces. However, erupts only in about one million year period around 30Ma (Abbate et al., 2015). According to Ebinger et al (1993) the eruption of the flood basalts underwent in two distinct phases. They concluded that the first stage of eruption is to be from Eocene- Oligocene times and later around the mid-Miocene relatively more voluminous eruption has occurred marking the second phase. There was prolonged time gap of eruptions after the flood basalts (Bonini et al 2005: Corti et al., 2010). The Guraghe basalts that date between 8.3 to 10.6 Ma cover these Oligocene basalts (WoldeGabriel et al., 1990; Bonini et al., 2005; Corti et al., 2010).

From 10-5Ma transitional basalts with few trachytic flows have been reported (Peccerillo et al., 2003). These Guraghe- Anchar basalts are characterized by fine grain texture exposed with more than 300m thickness (Agostini et al., 2011). The rate at which evolved products erupt in the CMER increased quite considerably between 320 and 170Ka most presumably because of continuous production of magma underneath (Hutchison et al., 2016). Pantelleritic ignimbrites whose age ranges in between 5 to 4.1 Ma are found on top of the Anchar basalts (Bonini et al 2005). According to Giday WoldeGabriel et al (1990) these pyroclastic materials are strongly welded and voluminous that may have erupted from a nearby huge caldera such as Awassa or the buried gademota caldera. These pantelleritic ignimbrites namely Nazret pyroclastics have been reported to be exposed more than 700m thickness Agostini et al (2011) and tends to cover most parts of the MER (Bonini et al., 2005 and Giday WoldeGabriel et al., 1990). The chilalo trachyte that dates from 1.6 to 3.5Ma which also includes basaltic lava flows are overlain on the Nazret pyroclastics (Giday WoldeGabriel et al., 1990). The Bora Bericha rhyolitic unit that includes peralkaline trachytes can be well correlated with those of chilalo trachytes (Agostini et al., 2011). Recent basaltic lava flows erupted along the Wonji fault zone around 1.6Ma (Giday WoldeGabriel et al., 1990). These rocks usually form either lava flows or cinder cones orienting in the rift direction (Peccerillo et al., 2003). These fissural basalts associated with phreatomagmatic deposits are also observed on top of the Nazret pyroclastics (Di Paola, 1972).

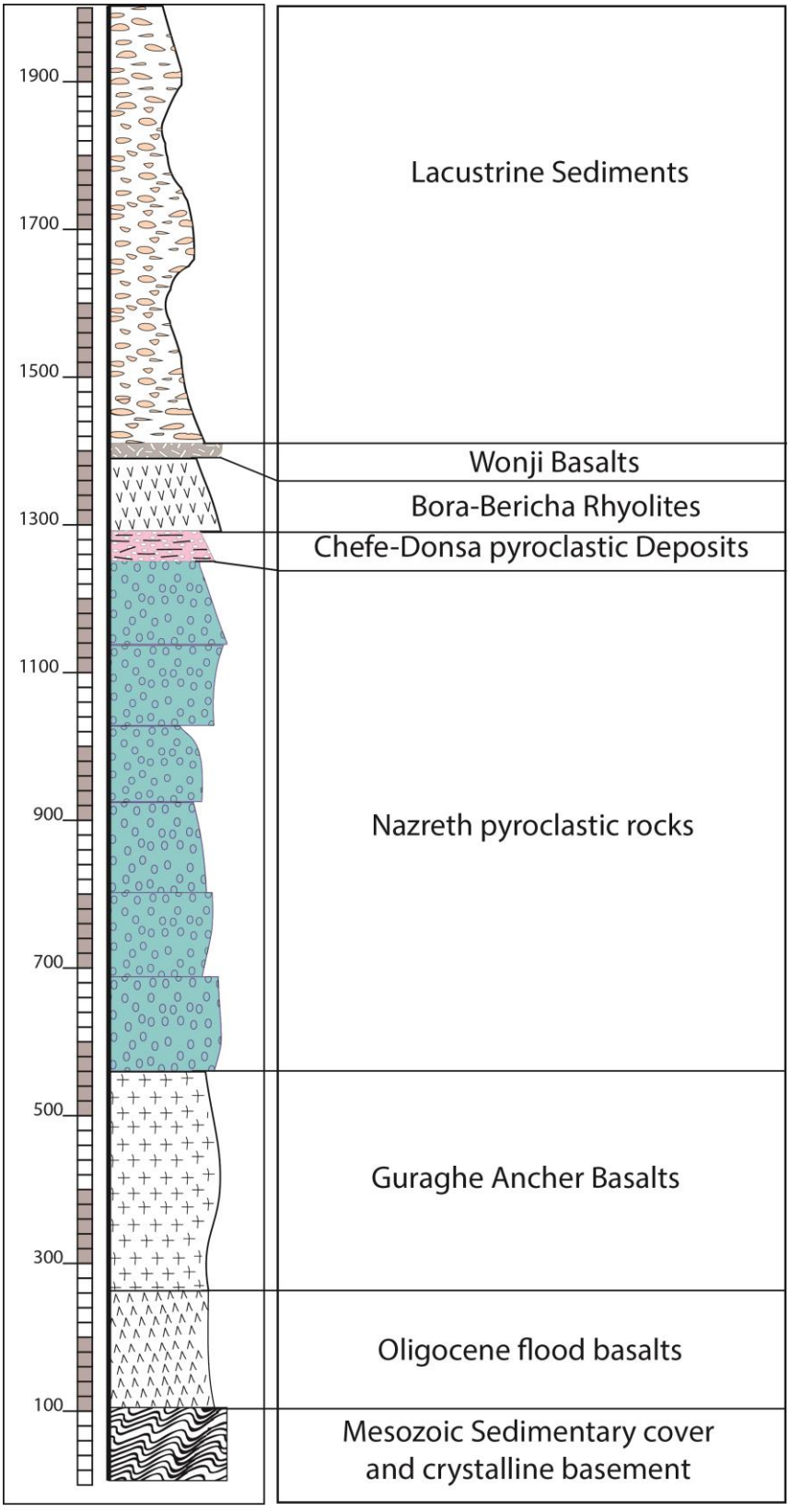

Figure 5. A schematic regional stratigraphy of the MER taken from section around the western escarpment of the Guraghe highlands around Kela village (modified after Agostini et al., 2011)

4. Research Methods

The research methods used to meet the objectives stated in chapter 1 are summarized below. Field observation of geological units in order to determine volcanic stratigraphy and tectonic structures in the study area has been done. Since substantial heat transfer is associated with magmatic chamber, investigation on the possible rock type associated with thermal conditions has been determined. This has been supported by petrographic methods to determine reservoir conditions. Fluid geochemical methods for estimating deeper temperatures have been used. Gas and water samples have been collected from the hot springs in the Butajira area. The hot springs are located near Ashute village. The criterion for selecting the location for sampling is based on spring temperature. Geothermometers such as cation geothermometer will be used for temperature estimation of the geothermal reservoir. The highest surface fluid temperature available has been taken. Clear hot springs that are not mixed with cold ground water were selected as much as possible. All the samples were filtered using 0.45 μm membrane and stored in a 250ml polyethylene bottles. Each sample was acidified with 2ml of HCl. The concentration of the acid is 0.02 since 2mg of powder HCl was stirred in 100ml of water. One of the most advanced and reliable means of identifying the deep heat source of a geothermal system is by using volatile elements like helium (Kennedy, 2000). The helium isotope ratio can be used to identify the source of heat whether it is from deep seated mantle plume or if it has an upper mantle or crustal signature. Thus by using noble gas chemistry, the heat source will be better defined and the provenance of volatiles can be established. For gas sampling from the hot springs we used 8-10mm sized funnels, gas-copper tubes, silicon tubes, clamps, clamp holder and plastic bottles necessary for sampling of the gases. There are two ways of sampling noble gases called flushing and displacement methods. In the flushing method the flow must be in only one direction as the procedure for sampling is given in figure 6. The copper tube which is plugged in a straight connection with the silicon tube is used to prohibit the diffusion of helium and will be sealed by crimping. The other sampling approach called the displacement method is used for swampy and inaccessible areas where the funnel will be filled with water by submerging it completely and then the funnel will be inverted displacing water with gas bubbles figure 7. Plotting softwares such as Arc GIS, Global mapper, Surfer and Grapher are also used for making maps, plots and stratigraphic sections.

4.1 Analytical techniques

Samples were collected at ten hot springs in the Butajira geothermal field. The samples were flushed for approximately an hour which significantly reduces the possibility of air contamination (after Hilton et al., 1990). Samples were analyzed in duplicates for two samples. They were analyzed at the Noble Laboratory of the University of Oxford using dual mass spectrometer. Gases were decanted from the SS cylinders and then an offline vacuum transfer line was used for sub-sampling in refrigerator-grade 10 mm outside-diameter Cu-tubes at <1.5 atm pressure. Titanium sponge held at 800˚C is used to remove the reactive gases and other hydrocarbons from the subsample in the purification line. In order to remove residual hydrogen, the titanium sponge was cooled to room temperature for about half an hour. The dual getter system of (SAES GP-50) held at 250˚c and (SAES NP-10) held at 25˚c are used to expand the gases. Hiden Analytical HAL-201 quadruple mass spectrometer was used for preliminary analysis. There are different cryogenic traps which are used for trapping various noble gas species. The stainless steel water trap held at 180K holds the gases where each was detached in their respective traps that were cooled by helium compressors. Helium was left over after neon and heavier volatiles were adsorbed at 31K and 15K in a charcoal and SS traps respectively. After helium was inlet in to Helix SFT mass spectrometer, neon was released and inlet into an ARGUS VI mass spectrometer when the temperature at the charcoal trap was raised to 90K. The three heavier elements were separated and inlets in to ARGUS VI by increasing the temperature at SS cryogenic trap to 300K. Re-adsorption on SS cryogenic trap held at 15K of heavy noble gases was followed by raising the temperature to 200K in order to transfer krypton and xenon in to the charcoal cryogenic trap that was held at 180K. To get rid of any residual argon, the extraction line was pumped for an additional of 15minutes. Then the temperature of the cryogenic trap was raised to 375K and remained for an hour so that krypton and xenon are released completely. After analyzing xenon in the ARGUS VI, then the left over gas was inlet in to ARGUS VI mass spectrometer for krypton analysis (after methods of Barry et al., 2016). The fluid samples were analyzed for noble gases by using 4200 MP-AES (Microwave Plasma Atomic Emission Spectrometry). Each component Na^{+}, K^{+}, Ca^{++} and Mg^{++} was calibrated at four standardized points with negligible error of 0.988. The samples were run in triplicate and the average values have been taken.

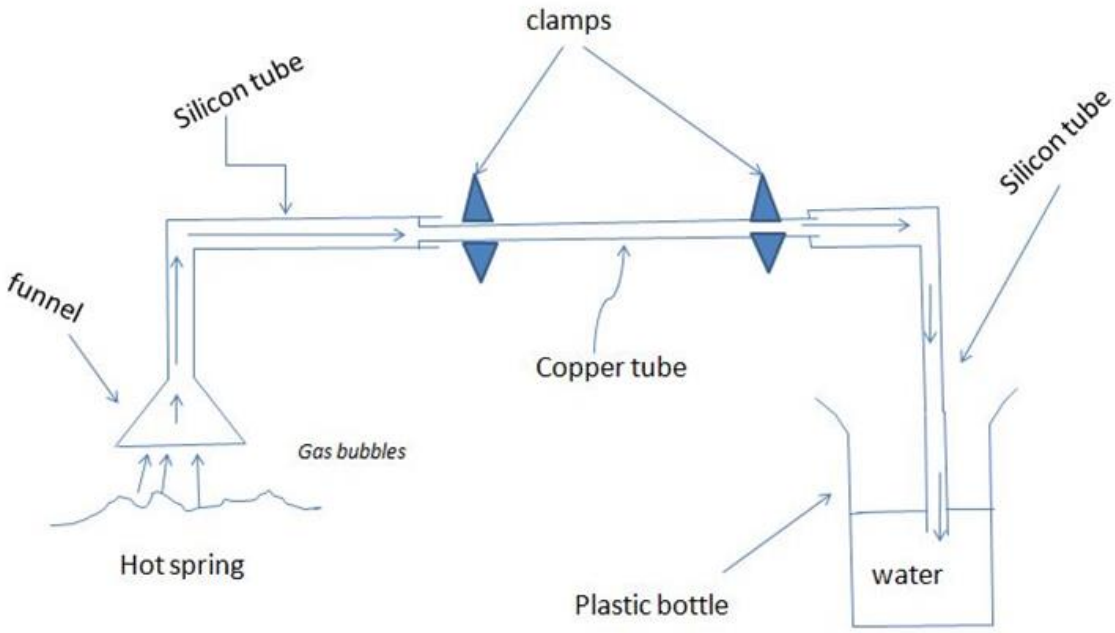

Figure 6. Sketch illustrating the procedure of gas sampling typically of flushing method

Figure 7. Gas sampling in the field at the top (flushing method) where prolonged flushing is conducted for approximately an hour and bottom (displacement method) where the funnel become submerged completely and the funnel will be inverted displacing water with gas bubbles

4.2 Theoretical Background of noble gas approach

One of the most reliable means for identification of the heat source is by using volatile elements like helium (Kennedy et al., 2000; Hristov et al., 2000; Barry et al., 2013; Breddam et al., 2000). Noble gases are considered as an efficient conservative fluid tracer because they are not affected by any chemical reactions due to their inert nature (Mazor et al., 1990; Ballentine et al., 1991; Graham, 2002; Ayache et al., 2015; Jackson et al., 2017). Noble gases also have unique isotopic signatures which are attributed to their respective origin(i.e., radiogenic vs. primordial), making them powerful tracers of volatile sources (Ballentine et al., 1991; Barry et al., 2013; Barry et al., 2015). Noble gases can originate from mantle, the atmosphere and from crustal sources (Hulston, 1994; Torgersen and Jenkins, 1982). There are two stable helium isotopes ^{3}He and ^{4}He where the former is primordial (i.e., leftover from when Earth accreted) from the mantle and the latter is produced from radiogenic decay of U and Th (Scarsi and Craig, 1996; Ayache et al., 2015). The existence of primordial ^{3}He also implies that previously trapped volatiles, during accretion, still reside in Earth's mantle (Graham, 2002). The existence of ^{3}He is typically associated with substantial heat transfer (Torgersen and Jenkins, 1982;

Kennedy et al., 2000; Roulleau et al., 2016). The process of radioactive decay of U and Th yields ^{4}He (Bottomley et al., 1984; Fueri et al., 2010; Graham, 2010). Thus the origin of volatile elements can be determined using helium isotopes (Barry et al., 2013). The measured sample $^{3}He/^{4}He$ ratio is typically designated as "R" expressed relative to the helium isotope ratio in the air abbreviated as "Ra" (= approximately 1.386×10^{-6}; Hulston, 1994). Each source of helium has a distinctive isotopic ratio for example magmatic helium is around 8Ra (i.e., 8 times the atmospheric value) and crustal helium is around 0.02Ra (Hulston, 1994; Torgersen and Jenkins, 1982; Furi et al., 2010; Barry et al., 2013; Barry et al., 2015: Breddam et al., 2000; Ayache et al., 2015).

Hydrothermal fluids are often magmatic in origin, as can be identified using helium isotopes in geothermal fluids. In this way the potential origin of the heat source can be determined (Torgersen and Jenkins, 1982). Because ^{4}He is produced by radioactive processes Kennedy et al (2000) the concentration of helium may increase as temperatures rise. However heat sources are typically associated with injection of higher $^{3}He/^{4}He$ fluids. Helium has previously been used to identify geothermal waters with high heat flow in Southern Bulgaria (Hristov et al., 2000). In this study the highest He concentrations were associated with proximity to faults. Since magma is also associated with enormous heat content, the existence of primitive helium (^{3}He) in the fluid can be used to infer communication between the magma and the geothermal fluids (Torgersen and Jenkins, 1982). Although helium isotope in geothermal fluids can be used to identify the source of heat, care needs to be taken during interpretation of such data. This is because of the occurrence of various processes that can have their own effect by either lowering or raising the isotopic ratio for example the presence of radioactive decay elements (Torgersen and Jenkins, 1982). The continuous production of alpha particles from radioactive decay elements like uranium and thorium can lower the isotopic ratio by the addition of radiogenic helium (Torgersen and Jenkins, 1982; Kennedy and Soest, 2007). The other is the solubility variation of volatile elements with mass which is certainly affected by temperature thus contributing the lost and/or addition of noble gases during exchange as the fluid ascends (Barry et al., 2016).

When geothermal fluid rise to the surface, the volatile elements originally associated with the fluid prefers to be in the steam phase instead of being in the liquid phase as hydrostatic pressure decreases. Thus analysis of the elemental ratio between elements with different

solubilities helps in determining mixing mode between the liquid and the steam phase (Mazor et al., 1990).

4.2.1 Mantle Source reservoirs

The structure of the mantle whether it is layered or unlayered even its historical evolution can be drawn using helium isotopes (Stuart et al., 2003). Mantle reservoirs such as Mid Oceanic Ridge Basalts (MORB) or the depleted MORB mantle (DMM) and Sub Continental Lithospheric Mantle (SCLM) are considered to have unique signatures of helium isotopes.

MORB-source

The helium isotope ratio of the MORB ranges from 7-9Ra suggesting a homogenous and well mixed upper mantle source (Furi et al., 2010; Barry et al, 2013). This helium isotope value originates from degassed magma from the well mixed upper mantle (Breddam et al., 2000). Thus $^{3}He/^{4}He$ ratios exceeding 7 times the ratio of air are assumed to have a significant mantle fraction (Mazor et al., 1990). The helium isotope ratio of MORB is relatively degassed versus primitive helium or plume signature (Gautheron and Moreira, 2002). The MORB, which typically representative of upper mantle signature, has uniform and homogenous R/Ra value of 8±1Ra indicative of depleted composition (Jackson et al., 2017). They further added that the depletion comes through prolonged circulation and withdrawal of substantial magma.

Plume-like sources

High helium isotope ratio within a range of 14 – 25Ra is representative of mantle hot spots (Torgersen and Jenkins, 1982; Stuart et al., 2003). Kennedy et al (2000) reports 32Ra for Hawaii hot spot. Highest $^{3}He/^{4}He$ ratio up to 50Ra has been measured from the basaltic lavas of the Baffin Island in Canada implying isolated primordial signature (Jackson et al., 2010). These high R/Ra values in various hot spot zones indicate a relatively undegassed plume source compared to the degassed MORB signature (Breddam et al., 2000). Furthermore, it is still been disputed, the presence of this primordial or relatively undegassed substance indicates the structure of the mantle to be layered and that it could not convect as a whole (Graham, 2002). The $^{3}He/^{4}He$ ratio is much higher at the center of the hot spot (Graham, 2002). Although it is commonly believed, from numerous data across several hot spots, that plumes have a very high $^{3}He/^{4}He$ ratio Jackson et al (2017) argues that the typical range that define plume source

can significantly be lower even from values below MORB signature. In general $^{3}He/^{4}He$ ratio from 5Ra to 50Ra can truly express the range of mantle plume source (Jackson et al., 2017).

SCLM sources

The SCLM is relatively colder and rigid than the underlying asthenosphere. This separated SCLM which is the uppermost portion of the mantle is also chemically distinct from the convecting asthenosphere (Barry et al., 2015; Gautheron and Moreira, 2002). The relatively less dense SCLM has been reported to be separated from the lower mantle for more than 1Ga which allows for developing its unique physical and chemical characteristics (Gautheron and Moreira, 2002). Although chemical interaction (metasomatism) can occur between fluids from the lower mantle and SCLM, where CO_2 and H_2O plays a role in transporting volatiles, the helium isotope ratio of SCLM (6.1± 0.9) is lower than the values of the MORB (Gautheron and Moreira, 2002).

4.2.2 Crustal systems

Helium isotope values within the range of 0.01- 0.1Ra are considered as typical signature of crustal systems (Torgersen and Jenkins, 1982). The production of radiogenic helium (^{4}He) from radioactive decay process is dominant in such systems. The hydrological system can also introduce crustal helium produced from weathered product of crustal rocks (Torgersen and Jenkins, 1982; Scarsi and Craig, 1996). Waters within the pore spaces in sedimentary rocks also could hold significant amount of radiogenic ^{4}He (Ayache et al., 2015). They also added that waters that are found within the continents will be more enriched in ^{4}He production than waters away from the continents since thick continental crust can supply substantial amount of crustal helium than the oceanic crust.

4.2.3 Atmospheric systems

Dissolved atmospheric helium can enter in to the geothermal system when meteoric water passes through fractures and in to the reservoir (Roulleau et al., 2016; Bosch and Mazor, 1988). Atmospheric noble gases are acquired in shallow aquifers during ground water recharge periods and can be transferred to other crustal reservoirs such as hydrocarbon deposits (Barry et al., 2016). Volcanic helium will not be significantly modified by helium derived from air since helium concentration in air is very small compared to other sources (Gautheron and Moreira, 2002).

4.3 Theoretical basis of geothermometers

Geothermometry is widely accepted as reliable method in estimating subsurface reservoir temperature (Wishart, 2015, Arnorsson, 2000). Fournier (1977) classify chemical geothermometers as being qualitative and quantitative. The qualitative geothermometers are mostly helpful for geothermal fields that are poorly constrained where no appropriate data is readily available. Mercury from stream sediments and volatile elements from the soil can predict the existence of old thermal manifestations (Fournier, 1977). The constituents of geothermal fluids are derived either by dissolution of primary minerals or from precipitation of secondary minerals (Arnorsson, 2000). These geothermometers provide numerical values and are regarded as quantitative geothermometers offering the least expected reservoir temperature (Fournier, 1977). Geothermometers can also be classified as solute, gas and isotope geothermometer (Arnorsson, 2000; Karingithi, 2009). Out of the major processes that occur when geothermal fluids rise to the surface is losing heat by conduction. Conductive cooling does not always change the chemical composition of the rocks. However, it will certainly influence the rate of saturation for minerals either by dissolution or by precipitation. The other process that changes the composition of the fluid is adiabatic cooling which occur during degassing by concentrating the solute in favor of steam loss (Arnorsson, 2000). In conditions where sub surface temperature is below the boiling temperature of the atmosphere, the temperature of the water that is coming out can be thoroughly considered as the aquifer temperature. If the formation temperature exceeds the atmospheric boiling temperature, then adiabatic cooling of the water will occur (Fournier, 1977). There are assumptions that require consideration in using geothermometers like for instance there is no conductive cooling and the system is considered to be adiabatic (Arnorsson, 2000; Karingithi, 2009; Murithi, 2012). According to Wishart (2015) there are other several assumptions to be considered in dealing with geothermometry such as the abundance of mineral constituents ascending to the surface vary rapidly and most importantly the chemical reactions governing the mineral species must be temperature dependent at specific depth. The other assumptions that require consideration is that there is no mixing with cold ground water and no re-equilibrium shall occur during ascent of geothermal fluid to the surface (Fournier, 1977). When subsurface temperature increases above 150°c equilibrium between minerals and solute can always be maintained. Migration of the fluid to the surface, degassing and dilution are among the major factors that led the

fluid not to be in a state of equilibrium (Wishart, 2015). There are two ways for calibrating geothermometers. One can be retrieved by doing experiments that determine equilibrium constant called theoretical and the other is from associating concentrations with their respective aquifer temperature (Arnorsson, 2000). Reservoir temperature estimation is given in accordance with depth Wishart (2015). Although equilibrium conditions can only occur within the reservoir, the application of geothermometry can at least tell the temperature at which equilibrium was last maintained (Arnorsson, 2000). Many equations have been devised by different scientists. An equation for a typical geothermometer reflects the temperature condition at which equilibrium was last achieved (Arnorsson, 2000; Battistel et al., 2014) There is a range of temperature where a typical mineral assemblage can be formed so knowing the mineral assemblage can tell at what equilibrium temperature that typical arrangement exists (Wishart, 2015). In order to identify equilibrated system from non-equilibrated, the application of various mineral equilibrium is essential (Arnorsson, 2000). The possibility of the rock to leaching during interaction with the water has an influence on achieving state of equilibrium. This is because it has direct impact in deciding the concentration of dissolved indicator elements (Fournier, 1977). The original temperature and the resident time of the water with in the reservoir and its flow rate play a great role for re equilibrium to exist (Fournier, 1977). Powerfully rising fluid is less affected by conductive cooling than slowly rising water which considerably loses heat (Fournier, 1977). There are two reactions which are exclusively dependent on temperature that governs the fundamental principle behind the application of geothermometers namely solubility and exchange reactions (Fournier, 1977).

The Na-K geothermometer

Although it is not necessarily true, the assumption that the chemical constituents are preserved within the water is the basis for the application of chemical geothermometry If equilibrium exists, ratio between cations can be used as geothermometer (Arnorsson, 2000, Fournier, 1977). Cation geothermometry, which is dependent on equilibrium ion reaction, especially the Na-K geothermometers is suitable for temperatures over 180˚c (WRC, 2013; Murithi, 2012). Fournier (1977) proposed range of temperature from 100˚c up to 200˚c. The ideal place of deposition for these feldspars is usually the up flow zone since their solubility increases with increasing temperature they have the tendency to precipitate during heat loss from the fluid either by boiling or through conduction

(Arnorsson, 2000). The process occurring in aqueous solution between feldspars is called exchange reaction (Arnorsson, 2000). As equilibrium temperature changes, the ratio between indicator elements also changes (Fournier, 1977). Na-K geothermometer depends on the detachment of Na and K from the aluminosilicates (Gulec,) The exchange reaction between Na and K is given below (after Arnorsson, 2000)

$$NaAlSi_3O_8 \text{ (albite)} + K^+ = KAlSi_3O_8 \text{ (K-feldspar)} + Na^+$$

Na-K geothermometer is widely accepted for estimating reservoir temperature for both felsic and mafic rock compositions (Arnorsson, 2000). It is well established, from previous researches, that the feldspars in low grade metamorphic rocks and hydrothermally altered rocks are microcline and albite respectively. Na-K geothermometer can provide reliable results for reservoir temperature above 100°c and for fluids with few calcium content (Karingithi, 2009; WRC, 2012). Although factors such as fluid residence time in the sub surface and temperature have effects in the estimation of reservoir temperature, Na-K geothermometer is still crucial since Na and K respond very slowly to re-equilibrate after cooling (Arnorsson, 2000).

5. Research Results

The results of this study include geological observations including description of lithological units and major tectonic structures and mainly geochemical data including noble gas isotopes and water geochemistry. These results are presented and discussed in the following sections considering also published and unpublished knowledge.

5.1 Geology of Butajira area

The Butajira area is comprised of various rock types as shown in the compiled geological map in figure 17. The Trap basalts of pre-rift formation are exposed on the western rift escarpment of the Guraghe highlands with more than 600m thickness. This succession serves as the major recharge zone for the Butajira geothermal system. Pyroclastic deposits including volcanic ash fall and ash flow deposits cover wide areas. These are mostly associated with lacustrine and alluvial sediments that include well rounded conglomerates, siltstones and sandstones. Highly crystal rich ignimbrites, most probably erupted from strongly evolved magma are exposed forming high topography ridges. The area is also covered by recent fissural basaltic lava fields that are associated with monogenetic scoria and cinder cones. In terms of tectonic structures a series of large normal faults trending NE/SW are found along the western rift escarpment. These faults cut and displace the pre-

rift basalts and ignimbrite formations. Recent faults of the WFB are aligned in NNE/SSW direction affecting the basalts and crystal rich ignimbrites of the rift floor. Small rhyolitic lava domes are also exposed in the southern sector of the study area.

5.1.1 Pre-rift basalts

A thick succession of basaltic lava flows are found exposed on the Guraghe highlands. These basalts were formed and deposited before the Ethiopian rift was initiated. This unit is typically correlated with 30Ma old flood basalts of north-central Ethiopia. According to Giday WoldeGabriel et al (1990) it is well exposed along the western rift escarpment reaching in thickness up to 900m. During the current study, an outcrop of columunar basalt is observed along a section. A thin reddish paleosoil layer that marks gap of deposition between different eruptions of this volcanics is observed. This unit underlies on the ignimbrites of the rift shoulder and it is characterized by aphyric texture. The other feature of this unit is that it is highly affected by weathering as shown in figure 8.

Figure 8. A. Pre rift basaltic formation from the western escarpment and **B.** exfoliation of highly weathered basalt from pre rift formation

5.1.2 Pre-rift ignimbrites

This pyroclastic unit is strongly welded and found covering the pre-rift basalts. Mostly it is made up of welded ash with few crystals and few lithic fragments. The distinct feature of this unit from the ignimbrites found within the rift is that it is characterized by large vesicles. This unit is affected by the rift boundary normal faults that formed the western escarpment at around 9.7Ma (WoldeGabriel et al., 1990).

Figure 9. Vesiculated ignimbrite with noticeable flow banding structure (top) and pre-rift ignimbrite affected by the border fault of the western escarpment (bottom)

5.1.3 Crystal-rich ignimbrite

This unit is characterized by light grey color and highly welded ash with big lithic fragments. Obsidian fragments are common as lithic materials. The crystals, mostly quartz and alkali feldspars are so abundant suggesting eruption from a crystal mush magmatic chamber which was highly depleted in melt but rather enriched in crystals. Mostly this unit is affected by faults that trend NNE/SSW.

5.1.4 Welded ignimbrite

This unit is exposed along river beds and channels that show remarkable flow banding structure with big lithics elongating in the direction of flow. This unit is relatively older than the crystal rich ignimbrite and it is more pumiceous than being enriched with crystals.

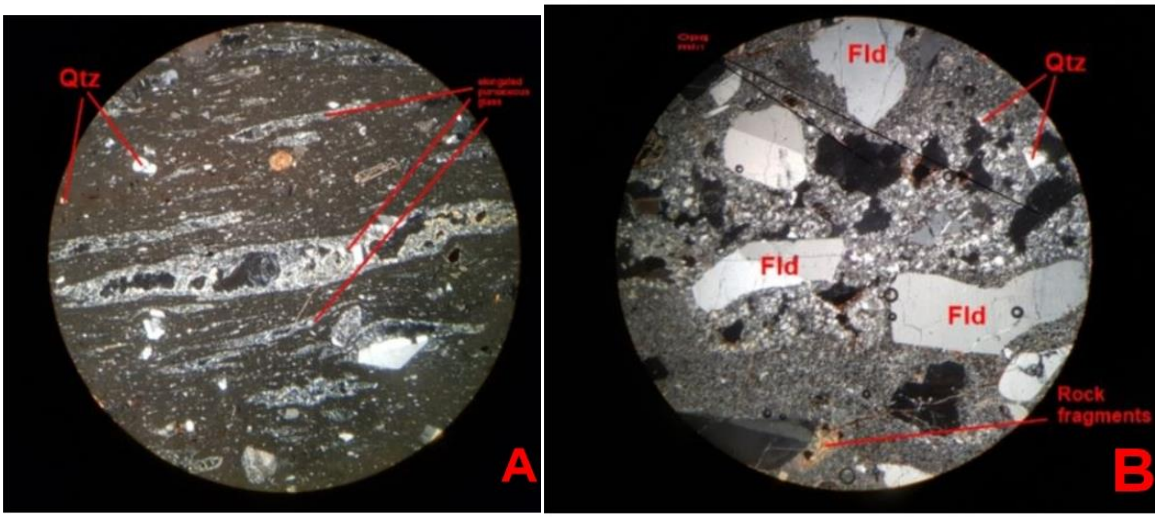

Figure 10. Pyroclastic deposit in XPL view with 4x magnification A= banded ignimbrite showing elongated pumaceous glass B= crystalline ignimbrite with quartz, alkali feldspars and rock fragments

5.1.5 Volcano-sedimentary unit

This unit mainly includes the widespread volcanic ash flow deposit that covers large parts of the area shown in the geological map in figure 17. This unit is also comprised with various clastic sedimentary rocks such as fine to a bit coarser sand stone, well sorted and laminated conglomerates. Usually these sedimentary units are found on top of the volcanic ash flow. The sandstone looks whitish to yellowish in color and reaches up to 5m in thickness. Silicified ash deposits are also found marking the process of interaction between hydrothermal fluids.

Figure 11. Pictures of laminated conglomerate deposit overlying on the ash flow deposit (left) stratified conglomerate in detail view (right)

The volcanic ash flow deposit has brownish to yellowish color. It is slightly welded and includes crystalline materials as lithics. Lithified or well laminated ash fall deposit overlies on this unit. Thick ash flow sections that reach up to 15m in height are observed.

Figure 12. Thick ash flow section (left) and ash flow overlying on top of welded ignimbrite (right)

5.1.6 Rhyolite lava

This unit is characterized by very fine grained texture and whitish in color. Rhyolite lava domes are found near Lake Abaya and further South of the study area. Since the lava is so viscous, it actually form dome structure. These lava domes are elongated toward NNE-SSW direction following the orientation of WFB trend. Flow banding structures are observed in this unit. Some are covered with pumaceous pyroclastic deposit. In terms of petrography quartz is predominant than pyroxene and alkali feldspars with few glasses in the matrix as shown in figure 14 and are named as quartz rich rhyolites according to modal classification and nomenclature using QAPF diagram (BGS, 1999).

Figure 13. Pictures of rhyolite lava with flow banding structures at river cut exposures.

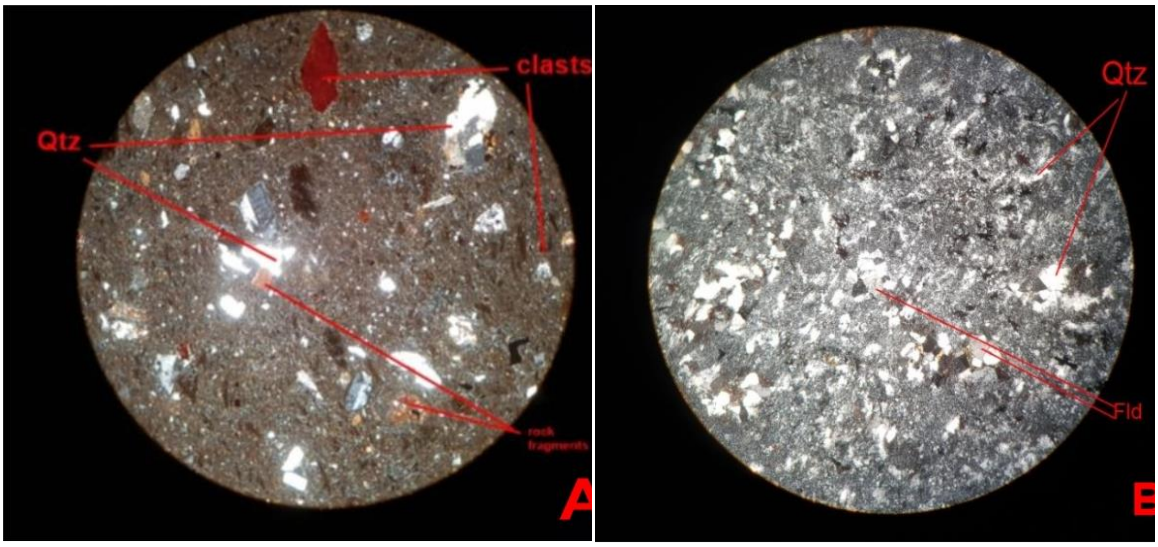

Figure 14. A= volcanoclastic material with several types of rock fragments of various origin **B=** quartz and alkali feldspar crystals of a rhyolite sample. Both photos are taken in XPL view and are 4x magnified

5.1.7 Recent basaltic lava flows and pyroclastic deposits

Basaltic lava flows and associated scoria and cinder deposits are the youngest volcanic product in the area. These lava flows are characterized by dark grey in color with large vesicles. The basalts of the rift floor are associated with fissural scoria cones which are aligned in NNE/SSW direction. These cones are moderately oxidized and are reddish in color. Often this unit intrudes the lithic dominated ignimbrite as dykes. These volcanic products are believed to erupt from monogenetic vents during the Quaternary (Bekele Abebe, 2015). These basaltic lava fields are so viscous they tend to flow only few kilometers from their vent. Large plagioclase crystals that show polysynthetic twinning are characteristic feature of this unit. Pyroxene and olivine among few alkali feldspar and quartz crystals has been observed. The basalts are highly vesiculated.

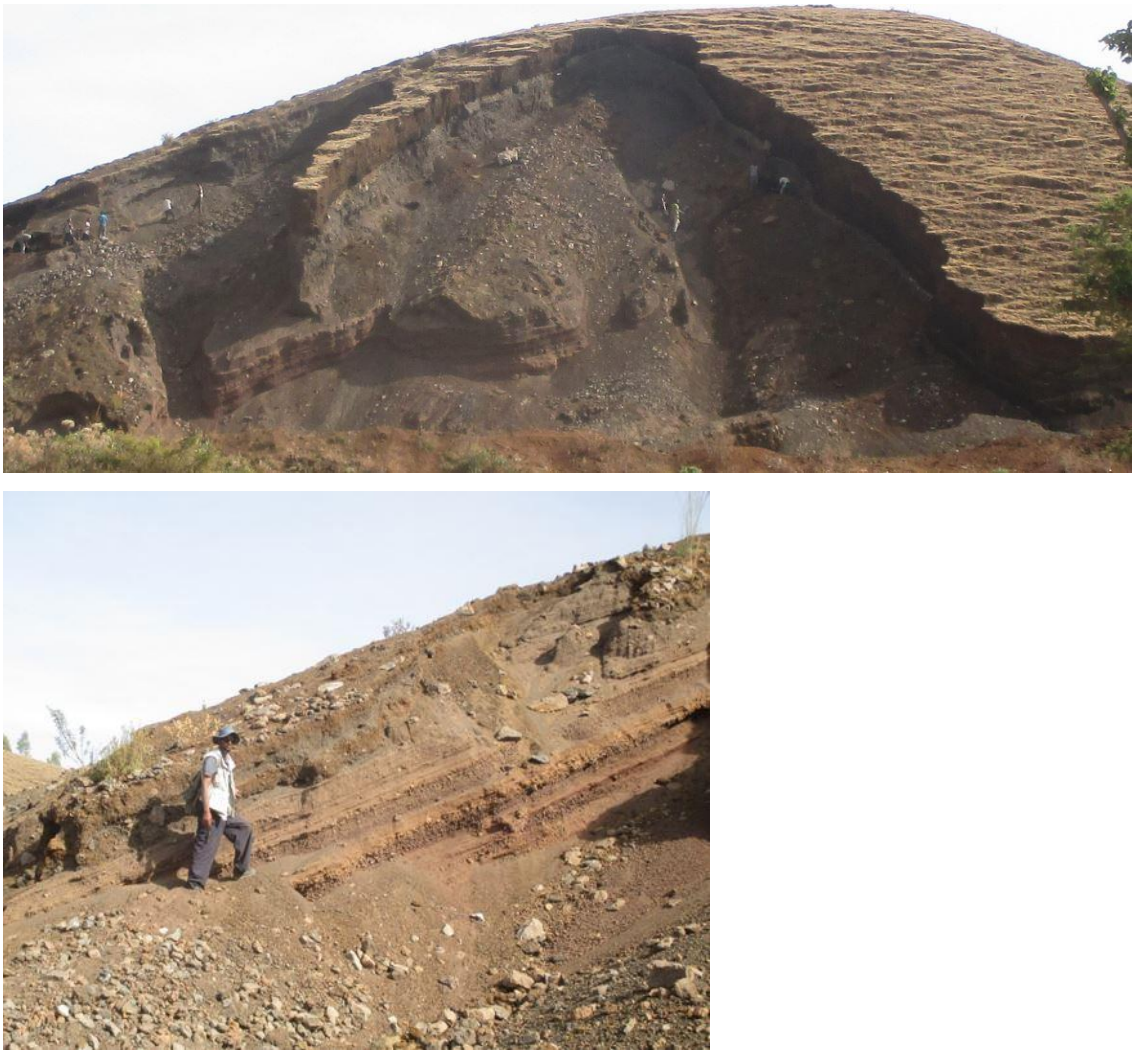

Figure 15. Scoria quarry site (above) and zoomed view of the same quarry (below)

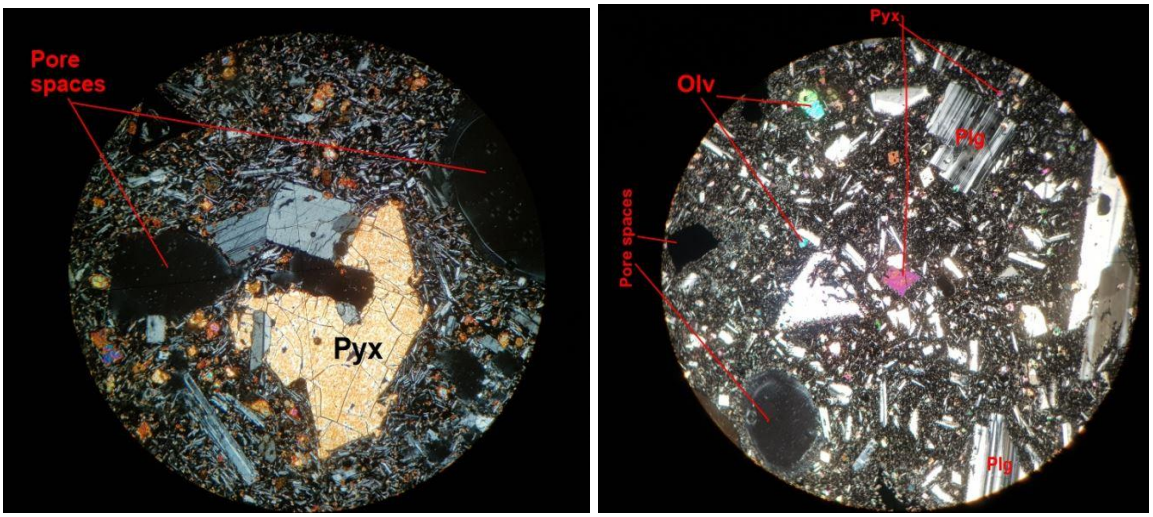

Figure16. Recent basaltic rocks in thin section showing pyroxene, olivine and plagioclase

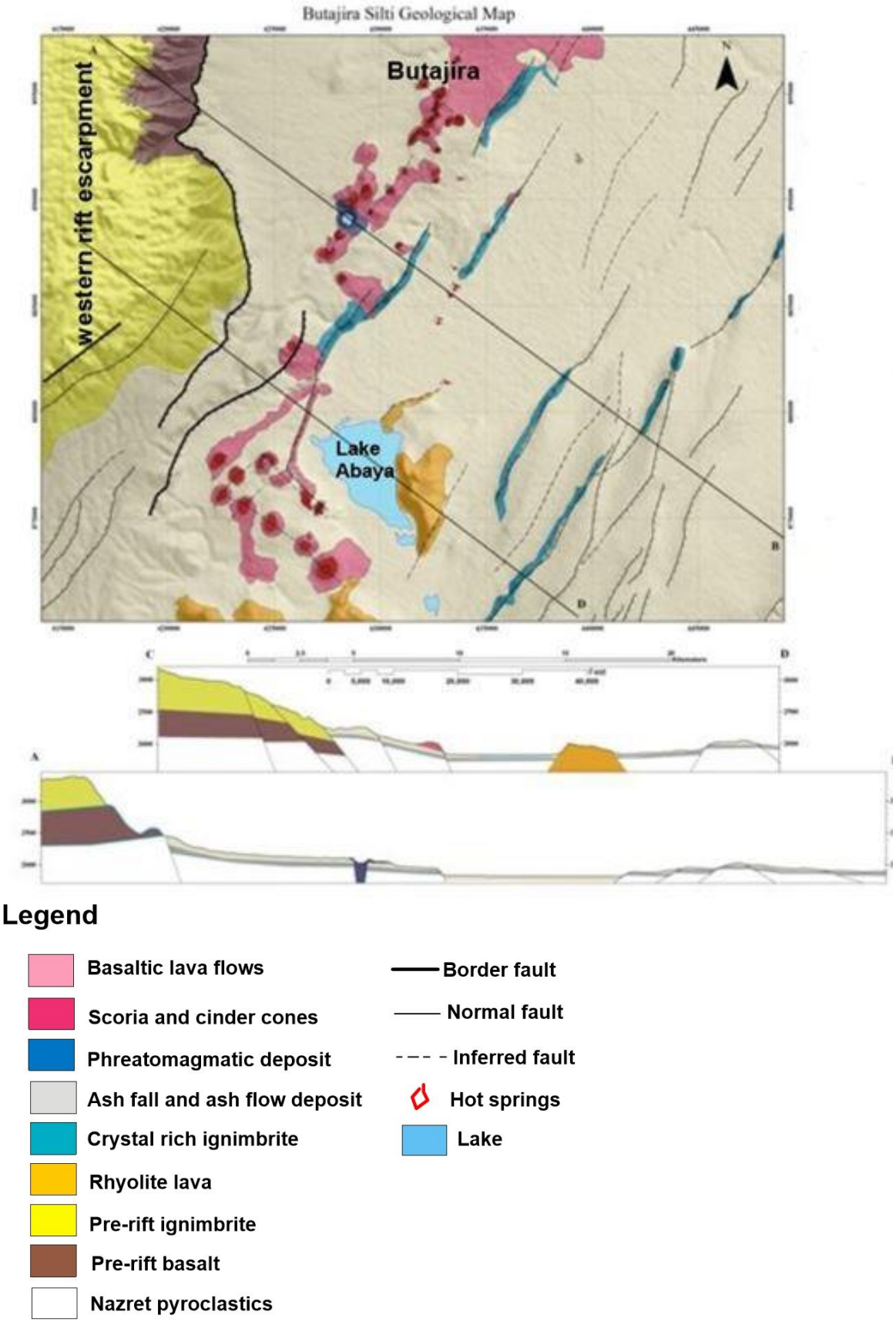

Figure 17. Geological map and cross section of the study area compiled using existing works (the unit Nazret pyroclastics has been inferred to be the geothermal reservoir from Agostini et al., 2011)

5.2 Geochemical Results

5.2.1 Noble gas results

The results of helium and neon isotope ratios are given in table 1. The value of helium isotope ratio is normalized and corrected for atmospheric helium entry either during sampling or during recharge mechanism. Accordingly R/Ra values ranging from 2.16 up to 2.43 with an average value of 2.29 have been obtained. Almost all the samples are considered to be representative samples as the air corrected value (Rc/Ra) of all the samples are broadly consistent with the measured R/Ra values with standard deviation of 0.085 as displayed in figure 18.

Table 1 Results of isotopic ratio of various noble gas species

Sample No	Temp (◦c)	$^{3}He/^{4}He$ (R/Ra)	Rc/Ra	$^{21}Ne/^{22}Ne$	$^{20}Ne/^{22}Ne$	$^{4}He/^{20}Ne$	X- value
Ash 1	66	2.25	2.25	0.0294	9.811	1367.37	4401.21
Ash 2	85	2.26	2.26	0.0295	9.832	1396.05	4493.56
Ash 3	35.5	2.35	2.35	0.0294	9.964	5524.71	17782.07
Ash 4	86	2.38	2.38	0.0298	9.770	2697.16	8681.5
Ash 5	45	2.18	2.19	0.0294	10.067	31.176	100.34
Ash 6	84	2.43	2.43	0.0293	9.950	310.04	997.96
Ash 7	47	2.24	2.24	0.0293	9.770	1425.73	4589.08
Ash 8	32	2.31	2.32	0.0289	9.713	57.04	183.6
Ash 9	85	2.30	2.30	0.0291	9.910	281.86	907.24
Ash10	53	2.16	2.17	0.0329	10.553	48.53	156.23

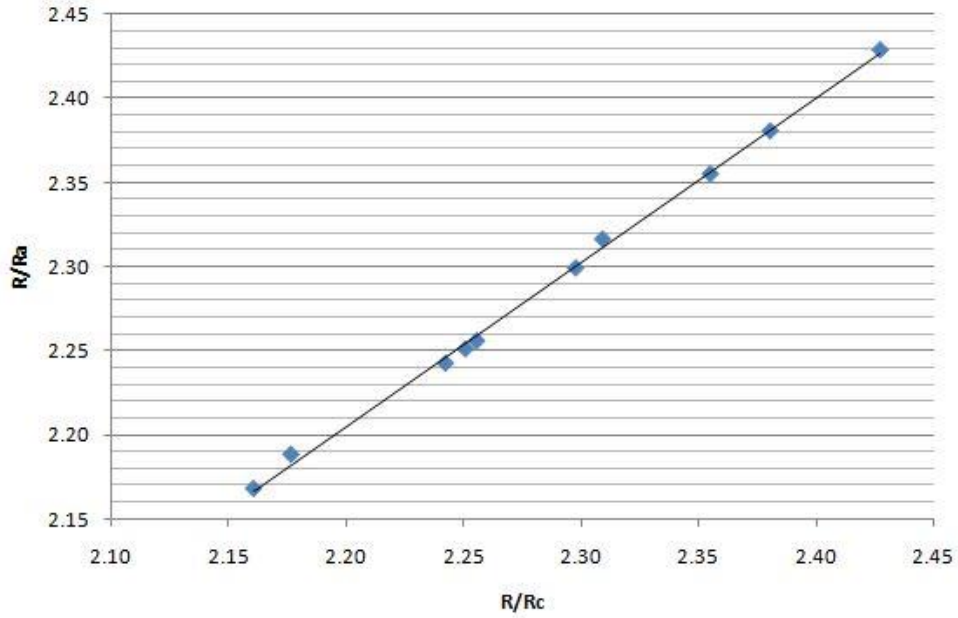

Figure 18. Linear plot for helium isotope ratios showing the consistency of all measured R/Ra values with air corrected values (R/Rc)

Moreover the outcome that may be encountered by air contamination was normalized using the X-factor where X-value = ($^4He/^{20}Ne$) measured/ ($^4He/^{20}Ne$) air× (βNe/βHe)], where β = Bunsen solubility coefficient (Barry et al., 2013; Fueri et al., 2010; Torgersen et al., 1982). Difference in temperature does not affect the solubility of neon significantly (Bottomley et al., 1984) and since the He/Ne ratio of all the other sources is considerably higher than He/Ne ratio of 0.29 of air, neon is commonly used for correction purposes (Torgersen and Jenkins, 1982; Hilton, 1996). X-values or He/Ne ratio of Butajira samples as shown in figure 19 shows a very high value reflecting an extremely negligible air contamination. The need for making air correction for calculated X-value above 10 is not quite important as it is not contaminated (Furi et al., 2010).

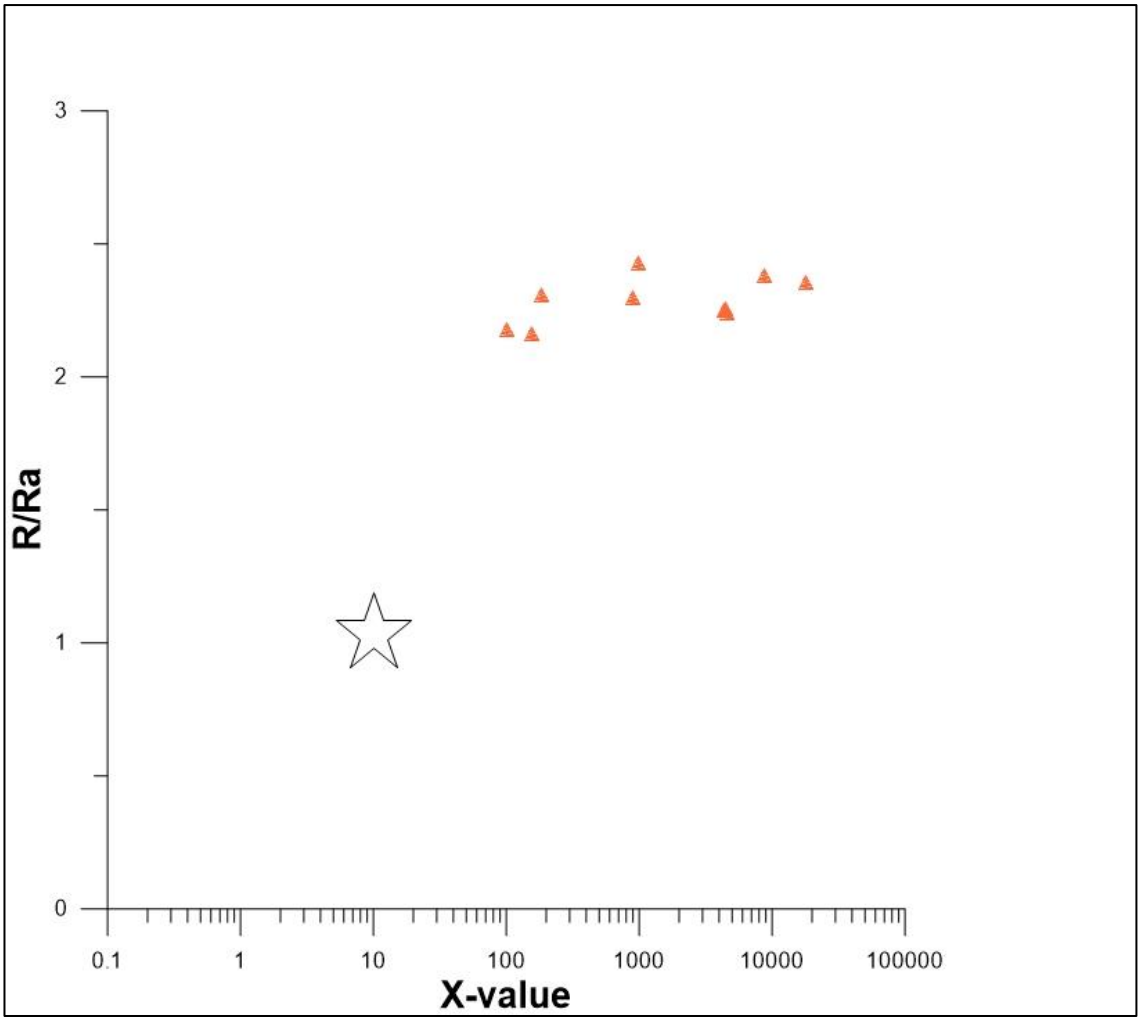

Figure 19. Plot of measured R/Ra values against X-value = (^{4}He/^{20}Ne)measured/(^{4}He/^{20}Ne)air×(βNe/βHe)], where β = Bunsen solubility coefficient (Barry et al., 2013; Fueri et al., 2010; Torgersen et al., 1982; Hilton et al., 1990). Isotope ratio of air is given in white star and orange triangles show the position of Butajira samples

5.2.2 Water geochemistry

There are numerous hot springs in the Butajira field all aligned in a NNE/SSW direction suggesting WFB orientation. Apart from determining the source of the fluid, the temperature of deep geothermal reservoir can also be provided numerically using molecular ratio (GSE, 2004). Among the common applications such as solute (water), gas and isotope geothermometry (Arnorsson, 2000), the water geothermometry is applied in this work. From various geothermometers, Na/K geothermometer, which is considered as one of the most reliable geothermometers (Wishart, 2015, Fournier, 1977, Fournier, 1979) has been selected and used in this research. Six hot spring samples have been taken and the results are shown in Table 2 and table 3.

Table 2 Estimated reservoir temperature of six cation samples calculated using the equation (after Arnorsson et al., 1998)

ID No	Location in (UTM) 37N		Elevation In (m)	Surface temperature in (˚c)	Concentration of cations in (ppm)				Estimated subsurface temperature In (c)
	Easting	Northing			**Na^+**	**K^+**	**Mg^{2+}**	**Ca^{2+}**	
C-1	433580	885955	1824	85	145.85	9.3147	2.8672	0.0921	145.85
C-2	433555	885919	1820	86	151.85	9.9387	4.1446	1.6205	151.85
C-3	434326	886670	1819	84	40.85	0.5931	0.4552	5.8098	40.85
C-4	432820	884392		86	96.85	2.0848	5.201	8.8847	96.85
C-5	432877	884579	1808	79	121.85	5.5916	0.9026	2.3047	121.85
C-6	433389	885734	1820	69.7	133.85	5.131	2.9141	3.3968	133.85

Table 3 Estimated reservoir temperature of six cation samples calculated using the equation (after Fournier 1977)

ID No	Location in (UTM) 37N		Elevation In (m)	Surface temperature in (°c)	Concentration of cations in (ppm)				Estimated subsurface temperature In (c)
	Easting	Northing			**Na^+**	**K^+**	**Mg^{2+}**	**Ca^{2+}**	
C-1	433580	885955	1824	85	145.85	9.3147	2.8672	0.0921	145.85
C-2	433555	885919	1820	86	151.85	9.9387	4.1446	1.6205	151.85
C-3	434326	886670	1819	84	40.85	0.5931	0.4552	5.8098	40.85
C-4	432820	884392		86	96.85	2.0848	5.201	8.8847	96.85
C-5	432877	884579	1808	79	121.85	5.5916	0.9026	2.3047	121.85
C-6	433389	885734	1820	69.7	133.85	5.131	2.9141	3.3968	133.85

Table 4 anion concentration of water samples from Butajira hot springs. Data taken from (GSE, 2017)

	Concentration of anions in (ppm)		
Sample No	Cl^-	HCO_3^-	SO_4^{2-}
1	79.9	1323.7	150.53
2	13.61	309.88	2.5
3	91.25	1426.18	188.36
4	143	2053.26	541.84
5	60.76	1150.46	141.42

6. Discussion

6.1 Interpretation of noble gas data

The measurement of $^{3}He/^{4}He$ can be used to infer for the possible source of heat since each sources, mantle or crustal, show distinguishable values (Barry et al., 2013). Interpretation of noble gas data needs to be made within the context of geological setting (Torgersen and Jenkins, 1982). The average helium isotope value of 2.3Ra suggests mixing between mantle derived signature and crustal contribution to the heat source and the consistency of this value within each samples, with standard deviation of 0.085 from the mean of the data, across the field suggests a single heat source. Results 7x above air imply mantle derivation (Mazor et al., 1990). Helium isotope values ranging from about 5-7Ra has been reported by Hilton (1996) to represent magmatic origin for the heat source also. If R/Ra values are less than the typical MORB values of (8±1Ra) but still above the value of atmospheric ratio of (1.4×10^{-6}), Torgersen and Jenkins (1982) concludes that the contribution of magmatic primordial helium is significant. The MORB value has been usually taken as a frame of reference for interpretation of such data (Hilton, 1996). When considering MORB value of 8Ra to represent 100 percent of mantle fraction and 0.02Ra for crustal sources, then the data for Butajira hot springs with an average of 2.3Ra will have 28% of mantle component and 72% of crustal sources. When assuming 20Ra to represent 100% of plume source and 0.02Ra for crustal origin, then 11.5% will imply plume signature while 88.5% indicates crustal source. It has been suggested by several authors that thermally buoyant plume intrudes the Ethiopian lithosphere around 30Ma which is responsible for the regional uplifting and dome formation by triggering the flood basalt magmatism (Chorowicz, 2005; Ring, 2014; Getahun Demissie, 2010; Wichura, 2010; Halldorsson et al., 2014; Abbate et al., 2014). Although there are some variations, high R/Ra values have been measured in several localities across the Ethiopian Rift and interpreted to imply significant lower mantle (plume) contribution (Scarsi and Craig, 1996). Butajira fluids with R/Ra values ranging from 2.16 to 2.43 imply significant lowering of this ratio. There are different processes that can cause this lowering. Although helium data is not affected by the addition of air, figure 21 shows the measured R/Ra values being plotted against $^{21}Ne/^{22}Ne$ in which Butajira samples fall outside the mixing line for crustal and mantle sources by the addition of atmospheric air as can be seen in the three neon isotope plot in figure 22 where most of the neon is dominated by air which is common in hydrothermal areas.

Analysis of helium isotopes alone may not always provide discernible results about the source of heat unless it is coupled with other noble elements (Halldorsson et al., 2014) Considering the source of the other noble gas species like neon is also significant in both determining the origin and provenance of volatiles. Easily distinguishable values of atmospheric neon, which is fractionated product of its original magmatic neon, and the involvement of these two in volcanic rocks helps in determining the provenance of the volatiles hence the source of heat (Graham, 2002). The theoretical solar neon is representative of accretionary neon (Graham, 2002; Halldorsson et al., 2014). The array that shows mixing line between plume like (solar), DMM, crustal and air like neon is given in figure 22. The three neon isotope plot of Butajira samples indicates air dominated neon which is typically anticipated in geothermal systems however three of the neon data are plotted along the plume - air trajectory supporting as an evidence for plume source.

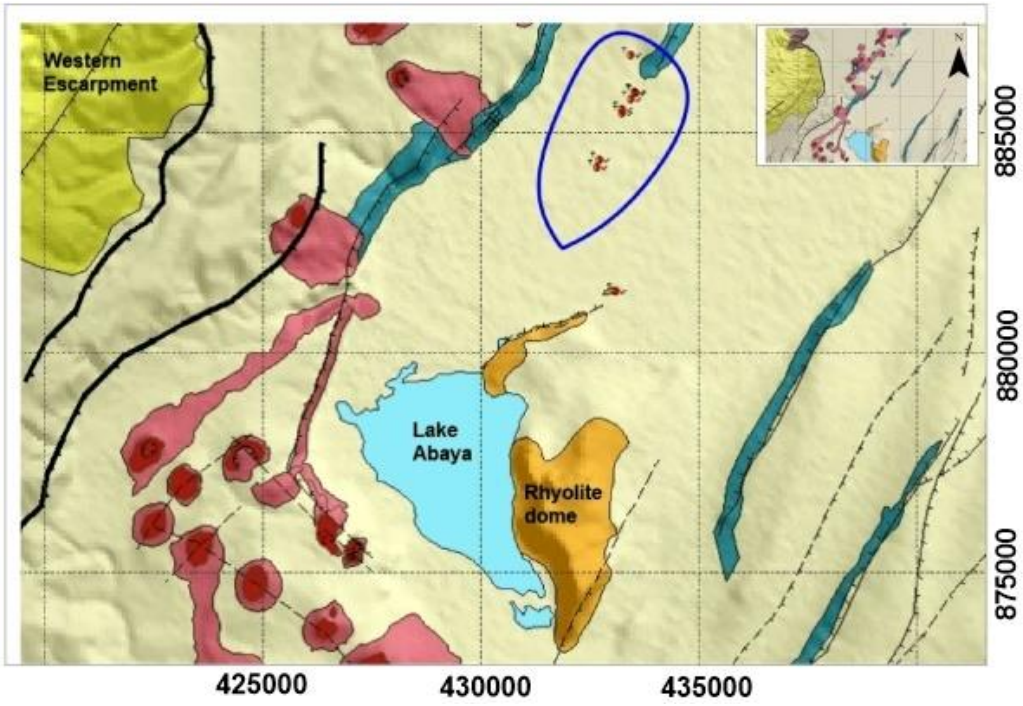

Figure 20. Geological map blue ellipse showing the location of the thermal manifestations and hence the sampling area. The most probable contributor of radiogenic helium (^{4}He) is shown few kilometers south of the manifestations forming rhyolite dome. The legend for the symbols is the same as in figure 17

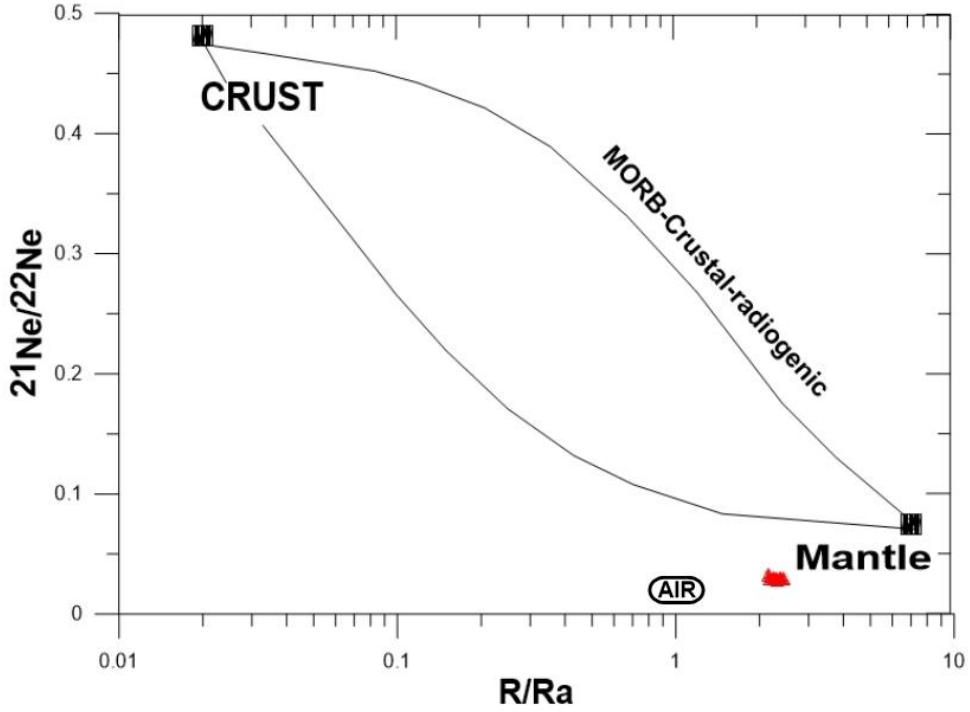

Figure 21. measured R/Ra values plotted against $^{21}Ne/^{22}Ne$ where the curved lines represent binary mixing between crustal (radiogenic) and mantle component (after Ballentine et al., 1996) Butajira samples are clustered in red polygon outside the mixing envelop due to addition of air

The lowering of the isotopic ratio of Butajira samples can be due to the production of ^{4}He more likely from crustal interaction. The rhyolite dome located 3km south of the sampling area which indicates magma chamber fractionating at shallow depth can supply alpha particles to the geothermal system. The contribution of evolved magma in supplying ^{4}He to the system plays significant role in lowering the overall R/Ra ratio (Torgersen and Jenkins, 1982). The interaction of primordial helium (^{3}He) with thick continental crust enriched in radiogenic helium (^{4}He) as the fluid ascends to the surface can also lower the ratio (Scarsi and Craig, 1996). Other than the long residence time of the magma chamber in the continent, the process of fractional crystallization can also accelerates the diffusion of primordial helium (^{3}He) to the surface hence lowering the ratio (Marty et al., 1996). The sampling area is found near the western escarpment of the MER where upwelling mantle plume that triggers volcanism around 30Ma is situated (Chorowicz, 2005; Getahun Demissie, 2010). The lowering of the helium isotope ratio can be caused from interaction and mixing between the deep rooted upwelling plume and upper mantle helium isotopes as well as crustal materials.

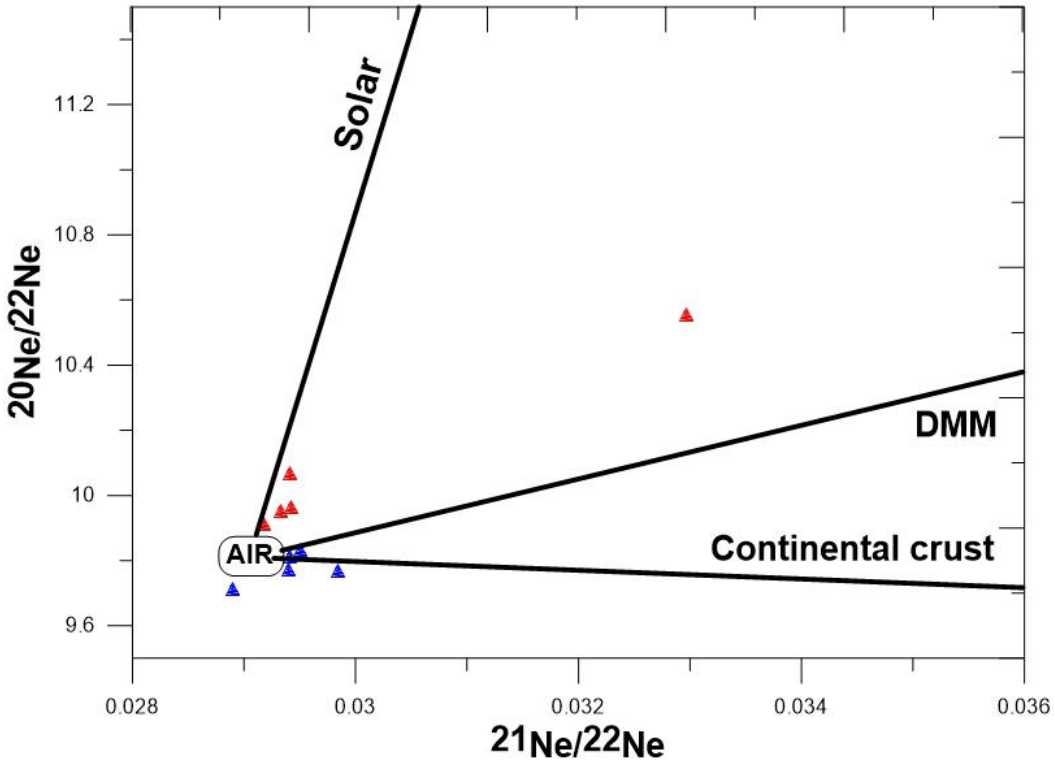

Figure 22. Three neon isotope diagram plotted along with DMM, Solar and crustal trajectories all intersecting air (after Halldorsson et al., 2014) most of the samples denoted by blue triangle are air dominated while red triangles are plotted along the plume (solar) trajectory

$^{3}He/^{4}He$ ratio less than 2.5Ra can be caused by significant radiogenic helium addition as the fluid ascends to the surface from water rock interaction (Hilton et al., 1993). Furthermore they added that ^{4}He addition and hence contamination of the primary fluid is common in regions of continental areas where R/Ra ratio much lesser than R/Ra of MORB can be thoroughly considered as an affective outliner of radiogenic helium. Scarsi and Craig (1996) also suggests that helium isotope ratio from 2-4Ra is certainly representative of radiogenic addition of ^{4}He and they argue that this effect is much higher in the rift margins than in the rift floor due to thickness variation of the continental crust along its boundaries. The source of heat that drives the geothermal system in Butajira is derived mainly from crustal sources. The measured value of 2.3Ra of Butajira samples is low relative to the MORB of 8Ra suggesting some crustal He entrainment. Several reasons may attribute for this lowering. One possibility of mixing and hence lowering of the ratio can be determined using binary mixing between crustal and mantle derived end member. Since both helium and neon of mantle derived component can be associated together interpretation using neon

data is quite important (Ballentine et al., 1996). Among these processes interaction and mixing between plume (lower mantle) and MORB (upper mantle) has been observed. Few Butajira samples are plotted very close to the solar trajectory which is considered as supporting evidence for primordial neon component rather than radiogenic neon. Data from Fernandina volcano of the Galapagos hot spot have also been interpreted to align along the solar line (for example; Kurz et al., 2009). Helium isotope ratio of 2.5Ra has been reported as relatively contaminated mantle (Yuce and Taskiran, 2013). Butajira samples are plotted in figure 23 against all the major heat contributing end members being aligned to the contaminated mantle curved line. Furthermore the occurrence of magmatic helium (^{3}He) in Butajira samples and its consistency in each sample that has been analyzed indicate a single heat source. Samples with helium ratio < 2Ra has been interpreted as being substantially degassed and contaminated character (Graham, 2002). In fact a very high ^{3}He/^{4}He value is not necessarily representative of mantle plume but rather indicates only the maximum end-member value (Jackson et al., 2017). Furthermore low ^{3}He/^{4}He values can be sourced from relatively cooler plume rather than upwelling hotter plumes (Jackson et al., 2017). The recent rhyolitic dome erupted from well evolved crustal magma chamber located south of the thermal manifestations is suggested as a heat source for the geothermal system of Butajira. This idea is supported by Samrock et al (2015) that proves the existence of substantial melt in the SDFZ at shallow crustal depths. The source of heat that drives the geothermal system in Butajira is derived mainly from crustal sources. The measured value of 2.3Ra of Butajira samples is low relative to the MORB of 8Ra suggesting some crustal He entrainment.

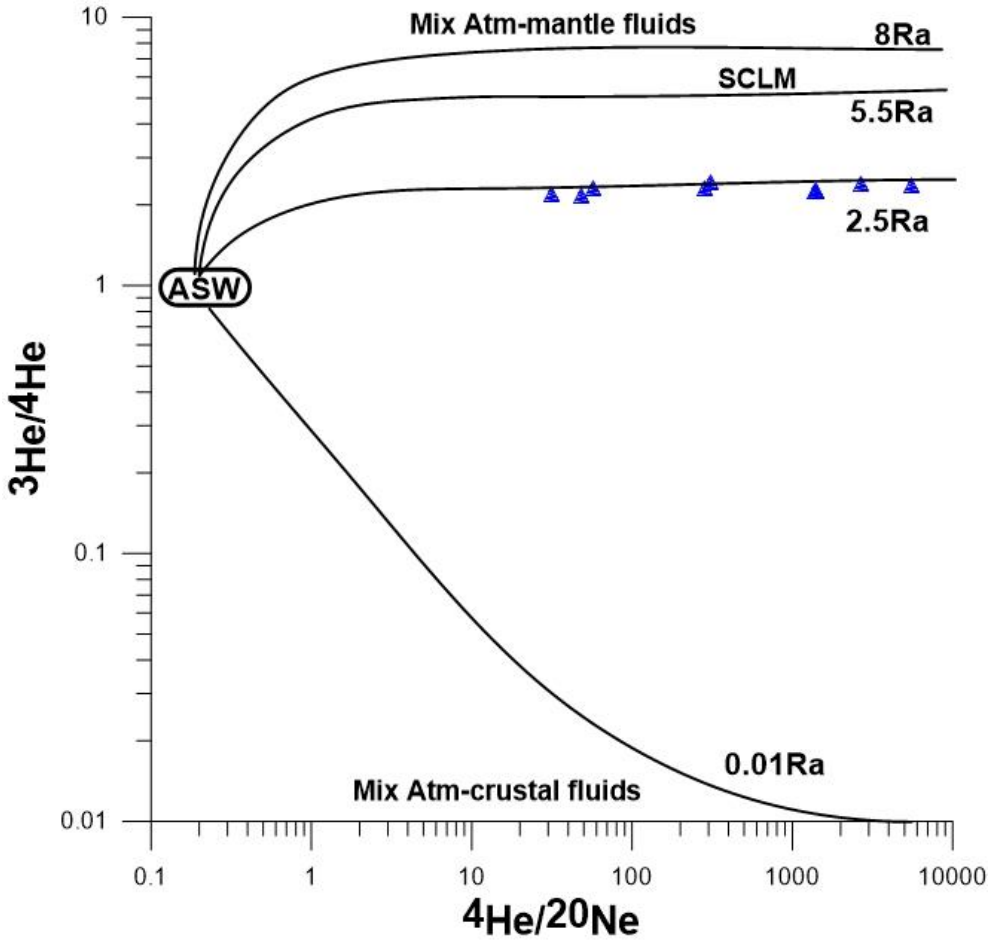

Figure 23. R/Ra values against 4He/20Ne to show binary mixing line between MORB, SCLM, crustal and air saturated water (ASW) (after Yuce and Taskiran, 2013) the blue triangles representing Butajira samples with an average of 2.3 Ra are plotted along the line that shows crustal contamination

6.2 Estimation of Reservoir temperature

The temperature of the hot springs at the time of collection lies from 69˚c up to 86˚c. Some geothermometers may either overestimate or underestimate subsurface temperature so comparison between various geothermometers is essential. Using Na/K geothermometer according to the equation proposed after Arnorsson et al (1998) and using the equation of Fournier (1977) reservoir temperature that ranges from 96˚c -151˚c and temperature ranging from 113˚c -173˚c respectively is determined for Butajira hot springs. The water type is considered as Na-HCO_3-SO_4 as plotted in figure 24. Among the six samples taken cat-ash 3 has been excluded from interpretation as the temperature estimated for the sub surface is much lower than the measured surface temperature. Any

sample whose estimated value is lower than the surfacial value is not representative sample (Yuce and Taskiran, 2013). This can be due to mistake during the acidification of the sample or during sample analysis. The samples are plotted as shown in figure 25 in the Giggenbach triangular diagram to proof whether or not rock water equilibrium exists in the aquifer. All the samples except cat-ash 3 are plotted and lie in the partial equilibrium zone. This shows some kind of mixing with cold ground water at the surface. The result obtained from Na-K geothermometer can be taken as reliable since it neither overestimates nor underestimates the reservoir temperature. Furthermore partial rock water equilibrium has been shown in figure 25. If all the samples lie in the immature zone and neither partial nor full equilibrium is maintained, then reliability in the result of the geothermometer will not be accepted (Yuce and Taskiran, 2013). However the temperature of the geothermal reservoir is expected to be higher than the estimated value obtained from using both equations proposed by Arnorsson et al (1998) and Fournier (1977). This is because it is common that the fluid temperature will decrease from its original value by the time it reaches to the surface (Arnorsson, 2000).

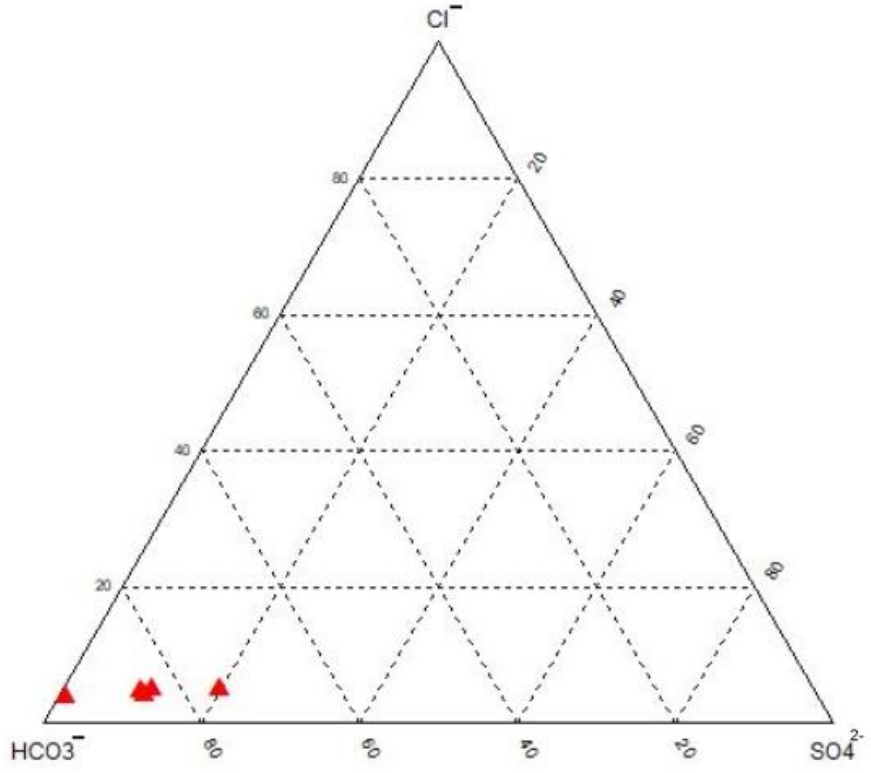

Figure 24. Ternary diagram of Cl-HCO_3-SO_4 red triangles that designates the samples are plotted close to the HCO_3 axes

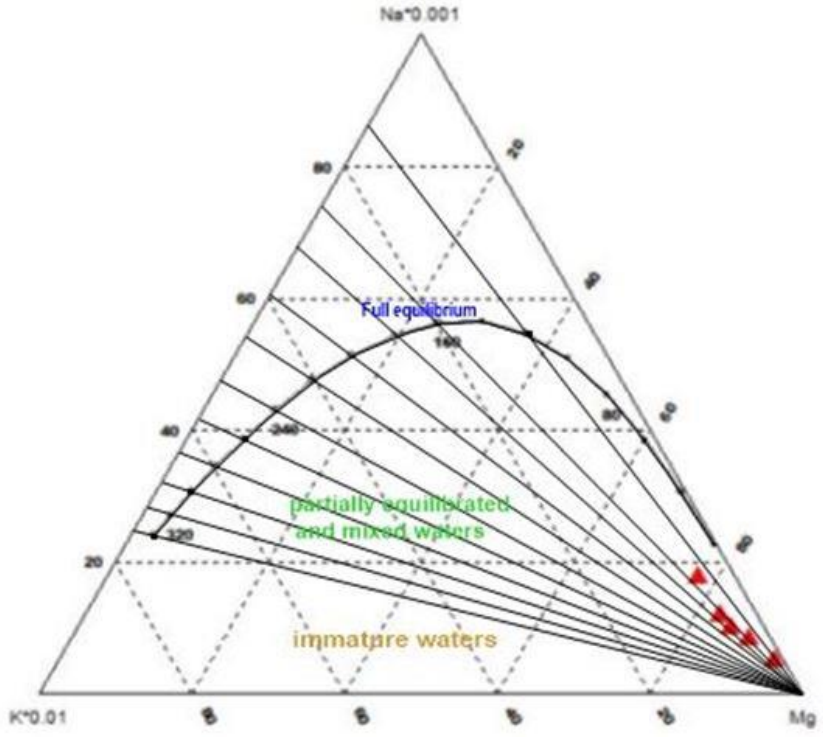

Figure 25. Na-K-Mg ternary diagram (after Giggenbach, 1988) red triangles indicate the samples plotted in the mixed and partially equilibrated zone.

The estimated temperature obtained from Arnorsson et al (1998) is above 150˚c while temperature estimated after Fournier (1977) is above 173˚c. Thus the sub surface temperature in Butajira geothermal field is at least certainly above 150˚c in temperature. The broad consistency of Butajira samples calculated both after the proposed equation by Arnorsson et al (1998) and Fournier (1979) are shown in figures 26 and 27 respectively. In fact the closeness of these values for the estimated temperature from the two equations gives reliability on the results obtained.

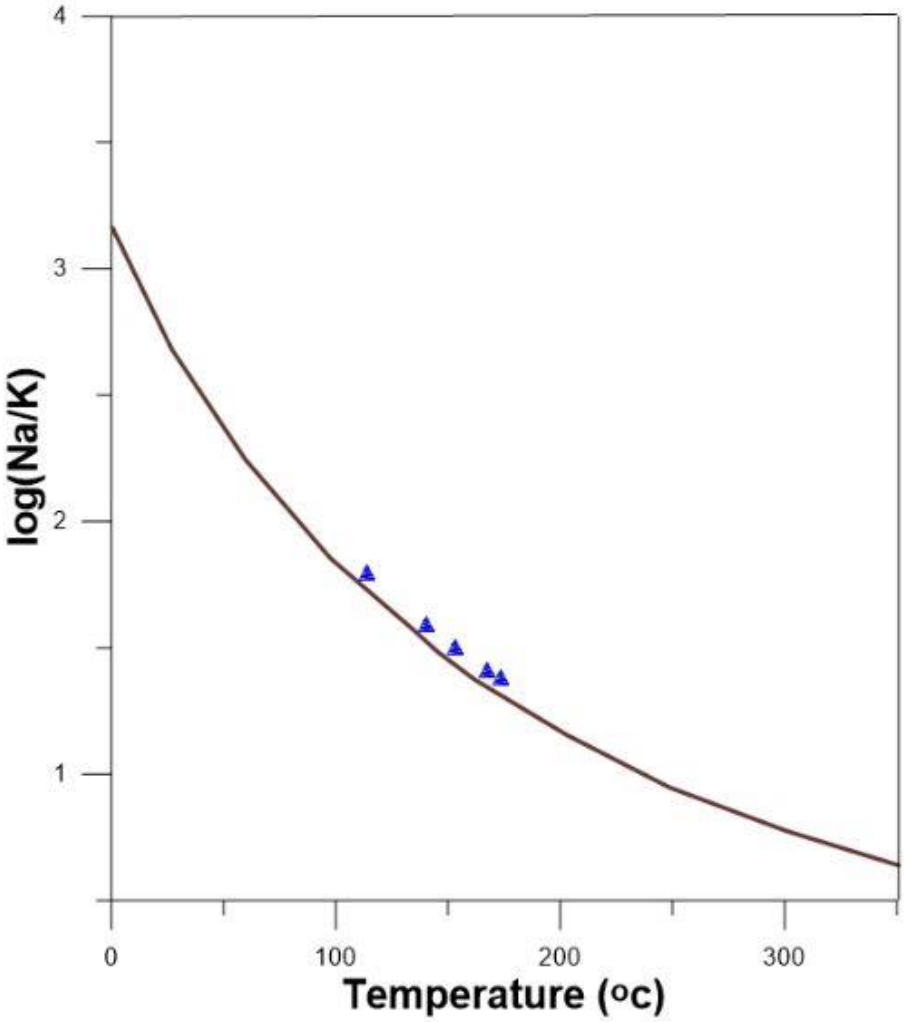

Figure 26. temperature curve for the Na/K geothermometer (after Arnorsson, 2000) the brown curve indicates the temperature curve line proposed by Arnorsson et al 1998 the blue triangles represent Butajira samples calculated using the equation after Arnorsson et al 1998

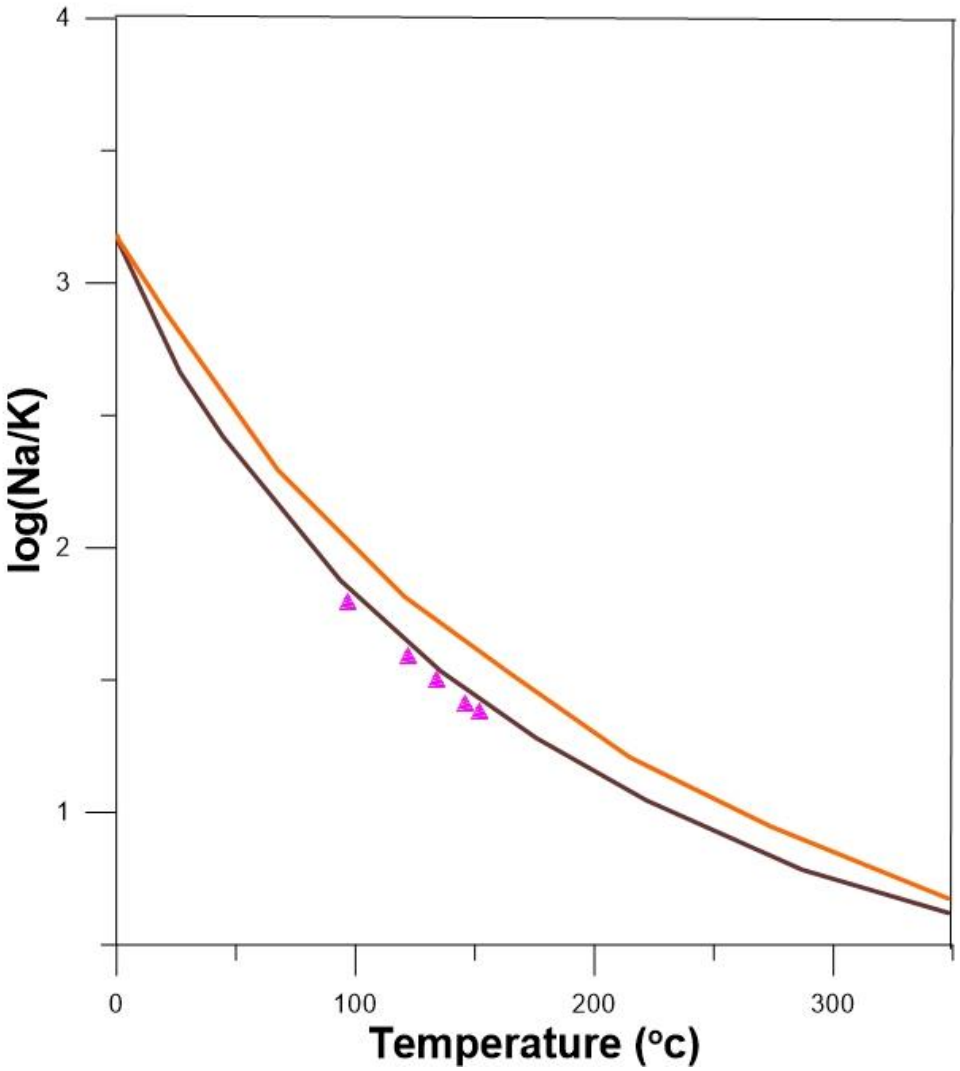

Figure 27. Temperature curve for the Na/K geothermometer (after Arnorsson, 2000) the brown curve is after Arnorsson et al 1998 while orange curve is obtained (after Fournier, 1979) the purple triangles represent Butajira samples calculated after the equation proposed by Fournier 1979

7. Summary

Preliminary conceptual geothermal model

Geothermal system is characterized by its main components such as recharge areas, elevated topographies suitable for enhancing ground water flow, geological structures that acts as fluid pathways, source of heat that provides heat to the system and impermeable lithological units to seal the direct upward flow of rising steam so that convective hydrothermal reservoir will be created. It has been argued that the formation as well as the propagation of the EARS in to which the Ethiopian rift is located has been controlled by pre existing structures of the Precambrian Era and this rifting was preceded by thermally buoyant plume (Getahun Demissie, 2010). The influence of transtensional component by forming en-echelon type WFB faults contributes for the propagation of rifting (Ameha Muluneh et al., 2014). In fact the regional stress field of the MOR of the Indian and Atlantic Ocean has also been reported to contribute for the development of the EARS (Min and Hou, 2018). This upwelling plume is believed to initiate from the core mantle boundary around 30Ma (Chorowicz, 2005; Ring, 2014). The high relief of Ethiopia as a consequence of dome formation and uplift of rift shoulders in both rift escarpments has been influenced by mantle plume activity (Chorowicz, 2005; Ring, 2014). Moreover active magmatism in the MER and the occurrence of high enthalpy geothermal prospects are certainly influenced by plume interaction (Getahun Demissie, 2010). The eruption of the flood basalt at relatively short period of time can be taken also as an evidence for the occurrence of magmatism and leaves its foot print for the present day topographical feature attained (Beccaluva et al., 2009; Hofmann et al., 1997). The deposition of the flood basalt in enormous volume covering very large area has been interpreted to be supplied from thermally buoyant mantle plume (Abbate et al., 2015). Although Breddam et al (2000) and Kennedy et al (2000) argues that high $^{3}He/^{4}He$ values above 32Ra are regarded to indicate lower mantle and/or plume signature Jackson et al (2017) argue that high $^{3}He/^{4}He$ ratio much above the ratio of MORB is not necessarily the typical value of mantle plumes. They rather conclude that it can only be taken to represent the possible maximum end member value. Hunt et al (2017) have showed that there is high CO_2 flux around the thermal manifestations in Butajira that shows good permeable zones. The consistency of the noble gas data indicates a single heat source. The heat source for Butajira geothermal fluids is derived predominantly from the crust where $^{3}He/^{4}He$ ratio is lower than the anticipated value of mantle plumes. This is because of interaction with crustal materials that can lower the ratio.

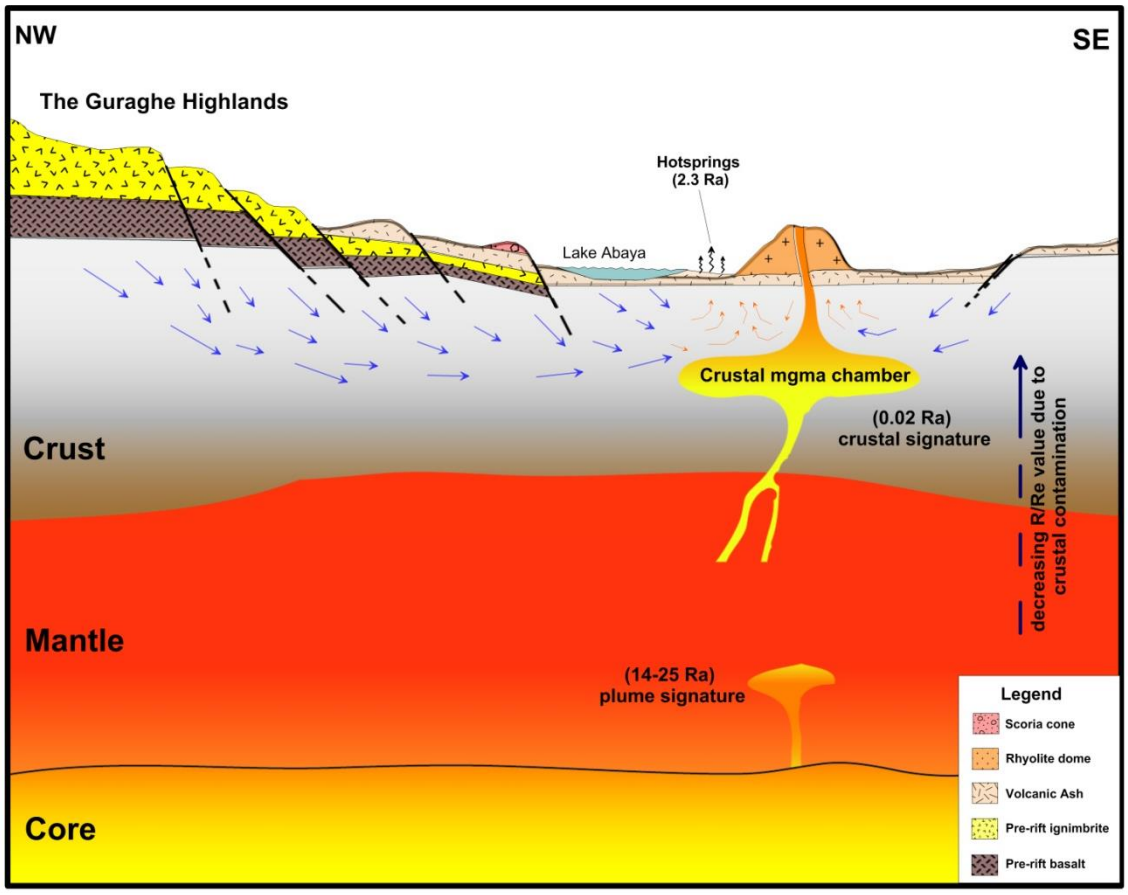

Figure 28. Preliminary conceptual geothermal model with lithological units and major tectonic structures. High R/Ra value of plume signature is continuously decreasing its ratio due to crustal contamination. The ratio of (14-25Ra) is taken from (Scarsi and Craig, 1996, $^{3}He/^{4}He$ = 0.02Ra is from Hulston, 1994 and $^{3}He/^{4}He$ = 2.3Ra is from this study)

The alignment of the Butajira thermal manifestations all discharging from NNE/SSW fault controlled permeability structures suggests the influence of faults in determining the fluid pathways. The Guraghe Highlands, with elevation more than 3000m asl, acts as the major recharge zone for the geothermal system where the fluids undergoes to the subsurface through faults and fractures. The fluids rise back to the surface after being heated. Although there is some kind of mixing between geothermal fluids with cold ground water as it ascends, the estimated reservoir temperature of Butajira field is well above 150°c. This has been shown by results obtained from Arnorsson et al (1998) and Fournier (1979) equations which are broadly consistent with each other. Figure 28 shows the upwelling mantle plume initiated at the core mantle boundary with R/Ra value from 14-25Ra indicating plume signature (Scarsi and Craig, 1996). This high $^{3}He/^{4}He$ ratio of plume origin gets

significantly lower up to 2.3Ra as recorded from the manifestations of Butajira. This is due to high crustal contamination most probably derived from radiogenic helium added from stagnant crustal magma chamber underneath the rhyolite dome near Lake Abaya as shown in figure 28.

Recommendation

The results of this study offer constraints on the heat source of Butajira geothermal field. This provides academical knowledge for the scientific community. Further works on alteration products is recommended. Drilling of appraisal geothermal wells for understanding the sub surface geology and to characterize the reservoir in detail is also recommended.

References

- Abbate, E., Bruni, P. and Sagri, M. (2015). Geology of Ethiopia: A Review and Geomorphological Perspectives, Springer
- Acocella, V., Tesfaye Korme., Salvini, F. and Funiciello, R. (2002). Journal of Volcanology and geothermal research. 2512: 1-15.
- Agostini, A., Bonini, M., Corti, G., Sani, F. and Manetti, P.(2011). Distribution of Quaternary deformation in the central Main Ethiopian Rift, East Africa, TECTONICS, VOL. 30, TC4010.
- Agostini, A., Bonini, M., Corti, G., Sani, F., Mazzarini, F. (2010). Fault architecture in the Main Ethiopian Rift and comparison with experimental models: Implications for rift evolution and Nubia–Somalia kinematics, Earth and Planetary Science Letters 301, 479–492.
- Ameha Muluneh., Cuffaro, M., Doglioni, C. (2014). Left-lateral transtension along the Ethiopian Rift and constrains on the mantle-reference plate motions. Tectonophysics
- Arnorsson, S. (2000). Isotopic and chemical techniques in geothermal exploration, development and use. IAEA, Austria, Vienna
- Ayache,M., Dutay, J.C., Baaptiste, P.J. and Fourre, E. (2015). Simulation of the mantle and crustal helium isotope signature in the Mediterranean Sea using a high-resolution regional circulation model. Ocean science.11: 965–978.
- Ballentine, C. J., O'Nions, R. K. and Coleman, M. L. (1996). A magnus opus heliun, neon and argon isotopes I a North Sea oil field. . Geochimica et Cosmochimica Acta 60: 831-849.
- Ballentine, C.J., O Nions, R.K., Oxburgh, E.R., Horvath, F. and Deak, J. (1991). Rare gas constraints on hydrocarbon accumulation, crustal degassing and groundwater flow in the Pannonian Basin. Earth and Planetary Science Letters. 105: 229-246.
- Barry, P.H., Hilton, D.R., Day, J.M.D., Fisher, J.F.P., Howarth, G.H., Magna, T., Agasher, A.M., Pokhilenko, N.P., Pokihilenko, L.N. and Taylor, L.A. (2015). Lithos. 216-217: 73-80.
- Barry, P., Hilton, D., Fischer, T., Moor, J., Mangasini, F. and Ramirez, C. (2013). Helium and carbon isotope systematics of cold "mazuku"CO2 vents and hydrothermal gases and fluids from Rungwe Volcanic Province, southern Tanzania.

- Barry, P.H., Hilton, D.R., Furi, E., Halldorsson, S.A. and Gronvold, K. (2004). Carbon isotope and abundance systematics of Icelandic geothermal gases, fluids and subglacial basalts with implications for mantle plume-related CO2 fluxes. Geochimica et Cosmochimica Acta. 134: 74–99.
- Barry, P.H., Lawson, M., Meurer, W.P., Warr, O., Mabry, J.C., Byrne, D.J. Ballentine, C.J. (2016). Noble gases solubility models of hydrocarbon charge mechanism in the Sleipner Vest gas field. Geochimica et Cosmochimica Acta. 194: 291–309.
- Bastow, I.D., Stuart, G.W., kendall, J.M. and Ebinger, C.J. (2000). Geophysics Journal International. 142: 000-000.
- Battistel, M., Hurwitz, S., Evans, W. and Barbieri, M. (2014). Multicomponent geothermometry applied to a medium-low enthalpy carbonate-evaporite geothermal reservoir. Energy Procedia. 59: 359 – 365.
- Beccaluva, L., Bianchini, G., Natali, C. and Siena, F. (2009). Continental Flood Basalts and Mantle Plumes: a Case Study of the Northern Ethiopian Plateau. JOURNALOF PETROLOGY 50: 1377-1403
- Bekele Abebe (2015). Fault Control on patterns of QuaternaryMonogentic vents in the Ethiopian Rift between Omo and Tendaho. SINET. 38; 00-00.
- Boccaletti, M., Bonini, M., Mazzuoli, R., Abebe Bekele., Piccardi, L and Tortorici, L. (1998). Quatemary oblique extensional tectonics in the Ethiopian Rift (Horn of Africa), Tectonophysics 287: 97-116
- Boccaletti, M., Mazzuoli, R., Bonini, M., Trua, T. and Bekele Abebe. (1999). Plio-Quaternary volcanotectonic activity in the northern sector of the Main Ethiopian Rift: relationships with oblique rifting, Journal of African Earth sciences, vol. 29, No. 4, pp. 679-698.
- Bonini, M., Corti, G., Innocenti, F., Manetti, P., Mazzarini, F., Abebe, T. and Pecskay, Z. (2005). Evolution of the Main Ethiopian Rift in the frame of Afar and Kenya rifts propagation, TECTONICS, VOL. 24, TC1007.
- Bosch, A and Mazor, E. (1988). Natural gas association with water and oil as depicted by atmospheric noble gases: case studies from the southeastern Mediterranean Coastal plain. Earth and Planetary Science Letters. 88: 338-346.
- Bottomley, D.J., Ross, J.D. and Clarke, W.B. Helium and neon isotope geochemistry of some ground waters from the Canadian Precambrian Shield. Geochimica n Cosmochimica Acta. 48: 1973-1985.

- Breddam, K., Kurz, M.D. and Storey, M. (2000). Mapping out the conduit of the Iceland mantle plume with helium isotopes. Earth and Planetary Science Letters. 176: 45-55.
- British Geological Survey (BGS) (1999). BGS rock classification scheme volume 1 classification of igneous rocks. Nottingham, UK
- Brotzu, P., Kazmin, V., Morbidelli, L., Piccirillo, E.M., Seife, M.B. and Traversa, G. (1979). Petrochemistry of the volcanics in the northern part of the Main Ethiopian Rift. In: Geodynamic evolution of the Afro- Arabian rift system, Rome, Italy
- Chorowicz, J. (2005). The East African rift system. Journal of African Earth Sciences 43: 379–410.
- Cornwell, D.G., Mackenzie, G.D., England, R.W., Maguire, P.K.H., Asfaw, L.M. and Oluma, B. (2006). Geological Society Of London. 259: 307-321.
- Corti, G. (2009). Continental rift evolution: From rift initiation to incipient break-up in the Main Ethiopian Rift, East Africa, Earth-Science Reviews 96: 1–53
- Corti, G., Manetti, P., Tsegaye Abebe., Bonini, M. and Mazzarini, F. (2010). THE VOLCANO-TECTONIC ACTIVITY OF THE MAIN ETHIOPIAN RIFT (EAST AFRICA): INSIGHTS INTO THE EVOLUTION OF CONTINENTAL RIFTING.
- Corti, G., Sani, F., Philippon, M., Sokoutis, D., Willingshofer, W. and Paola Molin. (2013). Quaternary volcano-tectonic activity in the Soddo region, western margin of the Southern Main Ethiopian Rift. TECTONICS, VOL. 32, 861–879.
- Deniel, C. (2009). Hetrogenous initial Sr isotope compositions of highly evolved volcanic rocks from the Main Ethiopian Rift, Ethiopia. Volcanology. 71: 495-508.
- Di Paola (1972). The Ethiopian Rift Valley. Pisa, Italy.
- Ebinger, C.J., T…Yemane., Giday WoldeGabriel., Aronson, J.L. and Walter, R.C. (1993). Late Eocene-Recent volcanism and faulting in the Southern Main Ethiopian Rift. Journal of the Geological Society. 150: 99-108.
- Fournier, R. O. (1979). Arevised equation for the Na/K geothermometer. Geothermal Resource Council. 3.
- Fournier, R. O. (1977). Chemical geothermometers and mixing models for geothermal systems. Geothermics.5: 41-50.
- Furi, E., Hilton, D.R., Halldorsson, S.A., Barry, P.H., Hahm, D., Fischer, T.P. and Gronvold, K. (2010). Apparent decoupling of the He and Ne isotope systematics of

the Icelandic mantle: The role of He depletion, melt mixing, degassing fractionation and air interaction. Geochimica et Cosmochimica Acta. 74: 3307–3332.

- Furman, T., Bryce, J. G., Karson, J. and Iotti, A. (2004). East African Rift System (EARS) Plume Structure: Insights from MaficLavas of Turkana, Kenya. JOURNAL OF PETROLOGY. 45: 1069–1088.
- Gasparon, M., Innocenti, F., Manetti, P., Peccerillo, A. and Tsegaye Abebe. (1993). Genesis of the Pliocene to Recent bimodal mafic-felsic volcanism in the Debre Zeyt area, central Ethiopia: Volcanological and geochemical constraints. Journal of African Earth Sciences. 17: 145-165.
- Gautheron, C. and Moreira, M. (2002). Helium signature of the SubContinental lithospheric mantle. Earth and Planetary Science Letters.199: 39-47.
- Geological Survey of Ethiopia (GSE) (2010). Geology of the Akaki Beseka area. Unpublished technical report, GSE, Addis Ababa, Ethiopia, 93pp.
- Geological Survey Of Ethiopia Hydrogeology, Engineering geology and Geothermal Department (GSE) (2004). Geochemical study of the Aluto-Langano Geothermal Field and the surrounding areas. Unpublished technical report, GSE, Addis Ababa, Ethiopia, 32pp.
- Getahun Demissie. (2010). Mantle Influence, Rifting and Magmatism in the East African Rift System (EARS) A Regional View of the Controls on Hydrothermal Activity**. In**: proceedings of world geothermal congress. Bali, Indonesia
- Gibson, I. (1972). The Chemistry and Petrogenesis of a Suite of Pantellerites from the Ethiopian Rift. Journal of Petrology. 13: 31-44.
- Giday WoldeGabriel., Aronson, J.L. and Walter, R.C. (1990) Geology, geochronology, and rift basin development in the central sector of the Main Ethiopia Rift. Geological Society of America Bulletin. 102: 439-458.
- Giday WoldeGabriel., Heiken, G., White, T. D., Asfaw, B., Hart, W. K. and Renne, P. R.,(2000). Volcanism, tectonism, sedimentation, and the paleoanthropological record in the Ethiopian Rift System, *in* McCoy, F. W., and Heiken, G., eds., Volcanic Hazards and Disasters in Human Antiquity: Boulder, Colorado, Geological Society of America Special Paper 345.
- Giordano, F., D'Antonio, M., Civetta, L., Tonarini, S., Orsi, G., Dereje Ayalew., Gezahegn Yirgu., Dell'Arba, F., Di Vito, M. and Isaia, R. (2014). Genesis and evolution of mafic and felsic magmas at Quaternary volcanoes within the Main Ethiopian Rift: Insights from Gedemsa and Fanta 'Ale complexes

- Graham, D.W. (2002). Noble Gas Isotope Geochemistry of Mid-Ocean Ridge and Ocean Island Basalts: Characterization of Mantle Source Reservoirs. Reviews in Mineralogy and Geochemistry. 47: 247-319.
- Graham, D (2010). Relict mantle from Earth's birth. Nature, News and Views
- Gupta, H and Roy, S. (2006). Geothermal Energy: An alternative resource for the 21ST Century, India, 293 pp.
- Halldorsson, S., Hilton, D., Scarsi, P., Tsegaye Abebe. and Hopp, J.(2014). A common mantle plume source beneath the entire East African Rift System revealed by coupled helium-neon systematics, Geophys. Res. Lett., 41, 2304–2311.
- Hilton, D. R., Gronvold, K., O'Nions, R. K. and Oxburgh, E. R. (1990). Regional distribution of He anomalies in the Icelandic crust. Chemical geology. 88: 53-67.
- Hilton, D. R., HammerSchmidt, S. T. and Friedrichsen, H. (1993). Helium isotope characteristics of Andean geothermal fluids and lavas. Earth and Planetary Science. 120: 265-282.
- Hilton, D.R. (1996). The helium and carbon isotope systematics of a continental geothermal system: results from monitoring studies at Long Valley Caldera (California, USA). Chemical geology. 127: 269-295.
- Hofmann, C., Courtillot, V., Feraud, G., Rochette, P., Gezahegn Yirgu., Ketefo, E. and Pik, R. (1997). Timing of the Ethiopian flood basalt event and implications for plume birth and global change. Nature. 389: 838-841.
- Hristov, V., Bojadgieva, K. and Benderev, A. (2000). DISSOLVED HELIUM AS INDICATOR FOR GEOTHERMAL WATER PROSPECTING. **In:** proceedings world geothermal congress. Kyushu- Tohoku, Japan, May28- June10.
- Hulston, J.R. (1994). The role of helium and other noble gases in the modelling of geothermal systems. **In:** proceedings 16th NZ geothermal workshop.
- Hunt, J. A., Amdemichael Zafu., Mather, T. A., Pyle, D. M. and Barry. P. H. (2017).Spatially Variable CO2 Degassing in the Main Ethiopian Rift:Implications for Magma Storage, Volatile Transport, and Rift- Related Emissions. Geochemistry, Geophysics, Geosystems

- Hutchison, W., Fusillo, R., Pyle, D.M., Mather, T.A., Blundy, J.D., Biggs, J., Gezahegn Yirgu., Cohen, B. E., Brooker, R.A., Barfod, D. N. and Calvert, A. T. (2016). A pulse of mid-Pleistocene rift volcanism in Ethiopia at the dawn of modern humans. Nature

- Hutchison, W., Mather, T., Pyle, D., Biggs, J. and Yirgu, G. (2015). Structural controls on fluid pathways in an active rift system: A case study of the Aluto volcanic complex. *Geosphere.* 11: 542–562.
- Jackson, M.G., Carlson, R.W., Kurz, M.D., Kempton, P.D., Francis, D. and Blusztajn, J. (2010). Evidence for the survival of the oldest terrestrial mantle reservoir. Nature. 466: 853-856.
- Jackson, M.G., Konter, J.G. and Becker, T.W. (2017). Primordial helium entrained by the hottest mantle plumes. Nature. 547.
- Kabeto, K., Sawada, Y. and Roser, B. (2009). Compositional Differences between Felsic Volcanic Rocks from the Margin and Center of the Northern Main Ethiopian Rift
- Karingithi, C. W. (2009). Chemical geothermometers for geothermal exploration. Unpublished report. Naivasha, Kenya.
- Kendall, J.M., Stuart, G.W., Ebinger, C.J., Bastow, L.D. and Keir, D. (2005). Magma assisted rifting in Ethiopia. Nature. 433.
- Kennedy, B., Fischer, T. and Shuster, D. (2000).'heat and helium in geothermal systems'. **In:** PROCEEDINGS, Twenty-Fifth Workshop on Geothermal Reservoir Engineering Stanford University, Stanford, California, January 24-26, SGP-TR-165.
- Kennedy, B.M. and Soest, M.C.V. (2007). Flow of Mantle Fluids Through the Ductile Lower Crust: Helium Isotope Trends. Downloaded from http://science.sciencemag.org/ on February 1, 2019.
- Keranen, K and Klemperer, S.L. (2007). Discontinuous and diachronous evolution of the Main Ethiopian Rift: Implications for development of continental rifts Earth and Planetary Science, Letters 265: 96–111.
- Kurz, M. D., Curtice, J., Fornari, D., Geist, D. and Moreira, M. (2009). Primitive neon from the center of the Galápagos hotspot. Earth and Planetary Science.286: 23–34.
- Mackenzie, G.D., Thybo, H. and Maguire, P.K.H. (2005). Crustal velocity structure across the Main Ethiopian Rift: results from two-dimensional wide-angle seismic modelling. Geophysics Journal International. 162: 991-1006.
- Macgregor, D. (2015). History of the development of the East African Rift System: A series of interpreted maps through time. Journal of African Earth Sciences. 101: 232-252.

- Maguire, P.K.H., Keller, G.R., Klemperer, S.L., Mackenzie, G.D., Keranen, K., Harder, S., O'Reilly, B., Thybo, H., Asfaw, L., Kahn, M.A. and Ameha, M. (2006). Crustal structure of the northern Main Ethiopian Rift from the EAGLE controlled-source survey; a snapshot of incipient lithospheric break-up. Geological Society Of London. 259: 269-291.
- Mahatsente, R., Jentzsch, G. and Jahr, T. (1999). Crustal structure of the Main Ethiopian Rift from gravity data: 3-dimensional modeling. Tectonophysics. 313: 363-382.
- Marty, B., Pik, R. and Gezahegn Yirgu. (1996).Helium isotopic variations in Ethiopian plume lavas: nature of magmatic sources and limit on lower mantle contribution. Earth and Planetary Science 144: 223-237
-
- Ministry of Mines and Energy (MOM) (1984). Compiled report on low enthalpy geothermal resources of Ethiopia. Unpublished technical report. Addis Ababa, Ethiopia
- Ministry of Mines and Energy (MOM) (2008). Investment Opportunities In Geothermal Energy Development: Tulu Moye Geothermal Prospect, Ethiopia. Unpublished technical report, MOM, Addis Ababa, Ethiopia.
- Min, Ge. And Hou, G. (2018). Geodynamics of the East African Rift System ~30 Ma ago: A Stress Field Model. Journal of Geodynamics. Accepted Manuscript for publication.
- Mazor, E., Bosch, A., Stewart, M.K. and Hulston, J.R. (1990). The geothermal system of Wairakei, New Zealand: physical processes and age estimates inferred from noble gases. Applied geochemistry. 5: 605-624.
- Mazzarini, F., Corti, G., Manetti, P. and Innocenti, F. (2004). Strain rate and bimodal volcanism in the continental rift: Debre Zeyt volcanic field, northern MER, Ethiopia, Journal of African Earth Sciences 39: 415–420.
- Minissale, A., Corti, G., Tassi, F., Darrah, T.H., Vaselli, O., Montanari, D., Montegrossi, G., Gezahegn Yirgu., Selmo, E. and Asfaw Teclu. (2017). Geothermal potential and origin of natural thermal fluids in the northern Lake Abaya area, Main Ethiopian Rift, East Africa. Journal of Volcanology and Geothermal Research. 336: 1-18.
- Mohr, P. (1962). The Ethiopian Rift System. Unpublished report. Addis Ababa, Ethiopia.

- Mohr, P. (1992). Nature of the crust beneath magmatically active continental rifts. Tectonophysics. 213: 269-284.
- Peccerillo, A., Barberio, M.R., Gezahegn Yirgu., Dereje Ayalew., Barbieri, M. and Wu, T.W. (2003). Relationships between Mafic and Peralkaline Silicic Magmatism in Continental Rift Settings: a Petrological, Geochemical and Isotopic Study of the Gedemsa Volcano,Central Ethiopian Rift, Journal of Petrology. **44**: 2003-2032.
- Pizzi, A., Coltorti, M., Bekele Abebe., Disperati, L., Sacchi, G. and Salvini, R. (2006). The Wonji Fault Belt (Main Ethiopian Rift): Structural and geomorphological constraints and GPS monitoring. The Geological Society of London. 259: 191-207.
- Ring, U. (2014). The East African Rift System. Austrian Journal of Earth Sciences 107/1: 132-146.
- Rooney, T. (2010). Geochemical evidence of lithospheric thinning in the southern Main Ethiopian Rift. Lithos. 117:33-48.
- Rooney, T., Furman, T., Bastow, I., Dereje Ayalew. and Gezahegn Yirgu (2007). Lithospheric modification during crustal extension in the Main Ethiopian Rift. JOURNAL OF GEOPHYSICAL RESEARCH 112: B10201.
- Rooney, T., Furman, T., Gezahegn Yirgu. And Dereje Ayalew. (2005). Structure of the Ethiopian lithosphere: Xenolith evidence in the Main Ethiopian Rift. Geochimica et Cosmochimica Acta. 69: 3889–3910.
- Rooney, T., Hanan, B.B., Graham, D.W., Furman, T., Blicheerttoft, J. and Schilling, J.G. (2012). Journal Of Petrology. 53: 365-389.
- Roulleau, E., Tardani, D., Sano, Y., Takahata, N., Vinet, N., Bravo, F., Munoz, C., Sanchez, J. (2016). New insight from noble gas and stable isotopes of geothermal hydrothermal fluids at Caviahue-Copahue Volcanic Complex: Boiling steam separation and water-rock interaction at shallow depth. Journal of Volcanology and Geothermal Research. 328: 70-83.
- Samrock,F., Kuvshinov, A., Bakker, J., Jackson, A. and Sintayehu Fisseha. (2015). 3-D analysis and interpretation of magnetotelluric data from the Aluto-Langano geothermal field, Ethiopia. Geophysical Journal International. 202: 1923-1948
- Scarsi, P and Craig, H. (1996). Helium isotope ratios in Ethiopian Rift basalts. Earth and Planetary Science. 144: 505-5 16.

- Solomon Kebede (2016). Country update on geothermal exploration and development in Ethiopia. In: Proceedings in the 6th African Rift Geothermal Conference. Addis Ababa, Ethiopia.
- Stuart, F.M., Evans, S.L., Fitton, J.G. and Ellam, R.M. (2003). High 3He/4He ratios in picritic basalts from Baffin Island and the role of a mixed reservoir in mantle plumes. Nature. 424: 57-59.
- Torgersen, T and Jenkins, W.J. (1982). Helium isotopes in geothermal systems: Iceland, The Geysers, Raft River and Steamboat Springs. Geochimica et Cosmochimico Acts. 46:739-748.
- Tsegaye Abebe., Balestrieri, M.L. and Bigazzi, G. (2010). The Central Main Ethiopian Rift is younger than 8 Ma:confirmation through apatite fission-track thermochronology. Terra Nova, 22: 470–476
- Tsegaye Abebe. (2000). Geological limitations of a geothermal system in a continental rift zone: example the Ethiopian Rift Valley. **In:** proceedings of world geothermal congress, Kyushu- Tohoku, Japan.
- Tsegaye Abebe., Mazzarini, F., Innocentti, F. and Manetti, P. (1998). The Yerer Tullu Wellel Volcanotectonic Lineament: a transtensional structure in central Ethiopia and the associated magmatic activity. Journal Of African Earthsciences.26: 135-150.
- United Nation Development Program (UNDP) (1973). Investigation of Geothermal Resources For Power Development. Geology, Geochemistry and Hydrology of hot springs of the East African Rift System within Ethiopia. Unpublished technical report, UNDP, New York.
- Utami, W.S., Herdianita, N.R. and Atmaja, R.W. (2014). The Effect of Temperature and pH on the Formation of Silica Scaling of Dieng Geothermal Field, Central Java, Indonesia**. In:** proceedings, Thirty-Ninth Workshop on Geothermal Reservoir Engineering Stanford University, Stanford, California, February 24-26, SGP-TR-202.
- Waikato Regional Council (WRC) (2013). The chemistry of waters of Te Aroha geothermal system. Unpublished technical report.
- Whaler, K.A. and Hautot, S. (2006). The electrical resistivity structure of the crust beneath the Northern Main Ethiopian Rift. The Geological Society of London. 259: 293-305

- Wichura, H. 2010. Topographic evolution of the East African Plateau:A combined study on lava-flow modeling and paleo-topography. Retrieved from http:// nbn-resolving.org/ urn: nbn: de: kobv:517-opus-52363.
- Wishart, D. (2015). Comparison of Silica and Cation Geothermometers of Bath Hot Springs, Jamaica W**I. In:** Proceedings World Geothermal Congress, Melbourne, Australia, 19-25 April.
- Wolfenden, E., Ebinger, C., Gezahegn Yirgu., Deino, A. and Dereje Ayalew. (2004). Evolution of the northern Main Ethiopian rift:birth of a triple junction. Earth and planetary science Letters 224: 213-228..
- Yuce, G. and Taskiran, L. (2013). Isotope and chemical compositions of thermal fluids at Tekman Geothermal Area (Eastern Turkey). Geochemical Journal. 47: 423-435.
- Zewde Gebregziabher. (1997). Ethiopian geothermal resources and their characteristics. Geothermal resources council transactions. 21